medRxiv preprint doi: https://doi.org/10.1101/2022.01.03.21268111; this version posted January 3, 2022. The copyright holder for this preprint (which was not certified by peer review) is the author/funder, who has granted medRxiv a license to display the preprint in perpetuity.
It is made available under a CC-BY-NC-ND 4.0 International license .

The hyper-transmissible SARS-CoV-2 Omicron variant exhibits significant antigenic change, vaccine escape and a switch in cell entry mechanism

Brian J. Willett*[1], Joe Grove*[1], Oscar A MacLean*[1], Craig Wilkie*[2], Nicola Logan*[1], Giuditta De Lorenzo*[1], Wilhelm Furnon*[1], Sam Scott *[1], Maria Manali*[1], Agnieszka Szemiel[1], Shirin Ashraf[1], Elen Vink[1], William Harvey [1], Chris Davis [1], Richard Orton[1], Joseph Hughes[1], Poppy Holland[3], Vanessa Silva[3], David Pascall[4], Kathryn Puxty[3], Ana da Silva Filipe[1], Gonzalo Yebra[5], Sharif Shaaban[5], Matthew T. G. Holden[5,6], Rute Maria Pinto[1], Rory Gunson[3], Kate Templeton[7], Pablo Murcia[1], Arvind H. Patel[1], The COVID-19 DeplOyed VaccinE (DOVE) Cohort Study investigators, The COVID-19 Genomics UK (COG-UK) Consortium*, The G2P-UK National Virology Consortium, The Evaluation of Variants Affecting Deployed COVID-19 Vaccines (EVADE) investigators, John Haughney**[3], David L. Robertson**[1], Massimo Palmarini**[1], Surajit Ray**[2] & Emma C. Thomson**[1,3,8]**

1. MRC-University of Glasgow Centre for Virus Research, UK, G61 1QH.

2. School of Mathematics & Statistics, University of Glasgow, UK

3. NHS Greater Glasgow & Clyde, Glasgow, UK

4. MRC Biostatistics Unit, University of Cambridge

5. Public Health Scotland

6. School of Medicine, University of St Andrews

7. NHS Lothian

8. London School of Hygiene and Tropical Medicine, London, UK

* Contributed equally to the publication

**Contributed equally to the publication

***Full list of consortium names and affiliations are listed in the appendix

Corresponding authors: Professor Emma Thomson and Professor Brian Willett, MRC-University of Glasgow Centre for Virus Research, UK, G61 1QH.

emma.thomson@glasgow.ac.uk and brian.willett@glasgow.ac.uk

NOTE: This preprint reports new research that has not been certified by peer review and should not be used to guide clinical practice.

medRxiv preprint doi: https://doi.org/10.1101/2022.01.03.21268111; this version posted January 3, 2022. The copyright holder for this preprint **(which was not certified by peer review)** is the author/funder, who has granted medRxiv a license to display the preprint in perpetuity.
It is made available under a CC-BY-NC-ND 4.0 International license .

Abstract

Vaccination-based exposure to spike protein derived from early SARS-CoV-2 sequences is the key public health strategy against COVID-19. Successive waves of SARS-CoV-2 infections have been characterised by the evolution of highly mutated variants that are more transmissible and that partially evade the adaptive immune response. Omicron is the fifth of these "Variants of Concern" (VOC) and is characterised by a step change in transmission capability, suggesting significant antigenic and biological change. It is characterised by 45 amino acid substitutions, including 30 changes in the spike protein relative to one of the earliest sequences, Wuhan-Hu-1, of which 15 occur in the receptor-binding domain, an area strongly associated with humoral immune evasion. In this study, we demonstrate both markedly decreased neutralisation in serology assays and real-world vaccine effectiveness in recipients of two doses of vaccine, with efficacy partially recovered by a third mRNA booster dose. We also show that immunity from natural infection (without vaccination) is more protective than two doses of vaccine but inferior to three doses. Finally, we demonstrate fundamental changes in the Omicron entry process *in vitro*, towards TMPRSS2-independent fusion, representing a major shift in the replication properties of SARS-CoV-2. Overall, these findings underlie rapid global transmission and may alter the clinical severity of disease associated with the Omicron variant.

medRxiv preprint doi: https://doi.org/10.1101/2022.01.03.21268111; this version posted January 3, 2022. The copyright holder for this preprint (which was not certified by peer review) is the author/funder, who has granted medRxiv a license to display the preprint in perpetuity.
It is made available under a CC-BY-NC-ND 4.0 International license .

Introduction

Protection against Severe acute respiratory syndrome coronavirus-2 (SARS-CoV-2) associated disease (COVID-19) is currently reliant on a range of vaccine technologies that induce immunity to the spike protein of the virus that first emerged in Wuhan city, China in 2019. Such early variant vaccines have become the cornerstone of the global public health response to SARS-CoV-2[1] but are threatened by the successive emergence of Variants of Concern (VOC) displaying increased transmissibility and/or evasion of adaptive immunity[2]. The evolution of SARS-CoV-2 variants with high transmission rates, increase the risk of the generation of variants of the virus with novel properties that may compromise this crucial element of the public health response. The balance between transmission advantage and immune evasion has resulted in the evolution of five VOCs that display these characteristics to varying degrees. The Beta (B.1.351 in Pango nomenclature) and, to a lesser extent, Gamma (P.1) variants were associated with immune evasion *in vitro* and spread locally but never dominated globally. In contrast, the Alpha (B.1.1.7) and Delta (B.1.617.2) VOCs attained a worldwide distribution and were responsible for significant waves of infections associated with an increase in reproduction number (R_0). Both variants harbour mutations at position 681 within the polybasic furin cleavage site (a histidine in Alpha and an arginine in Delta); changes associated with enhanced cell entry that likely confer an intrinsic transmission advantage. Alpha displayed lower immune evasion properties compared to Beta but higher transmission. Alpha was in turn replaced by the Delta variant that displayed more significant immune evasion in addition to enhanced furin cleavage[2–5].

Omicron is the fifth variant to be named as a VOC by the World Health Organisation (WHO) and the third (after Alpha and Delta) to achieve global dominance. The Omicron lineage (B.1.1.529) was first detected in mid-November 2021 in Botswana, South Africa[6] and quarantined travellers in Hong Kong[7]. It has split into three divergent sublineages (BA.1, BA.2 and BA.3) of which BA.1 has spread rapidly around the world. The BA.1 Omicron genome encodes 30 amino acid substitutions relative to Wuhan-Hu-1 within the spike glycoprotein (**Fig.1**), 15 of which are in the receptor-binding domain (RBD) and 9 within the receptor-binding motif (RBM), the RBD subdomain that interacts with the human ACE2 receptor. Six of these mutations (G339D, N440K, S477N, T478K, Q498R and N501Y) enhance binding affinity to the human ACE2 receptor. Combinations such as Q498R and N501Y may enhance ACE2 binding additively[8]. Overall, the Omicron RBD binds to the human ACE2 with approximately double the affinity (x2.4) of the Wuhan RBD[9]. Seven Omicron RBD mutations (K417N, G446S, E484A, Q493R, G496S, Q498R and N501Y) are associated with decreased antibody binding, importantly falling in epitopes corresponding to the three principal classes of RBD-specific neutralising antibodies.

medRxiv preprint doi: https://doi.org/10.1101/2022.01.03.21268111; this version posted January 3, 2022. The copyright holder for this preprint (which was not certified by peer review) is the author/funder, who has granted medRxiv a license to display the preprint in perpetuity.
It is made available under a CC-BY-NC-ND 4.0 International license .

Three deletions (amino acids 69-70, 143-145 and 211) and an insertion (at site 214) are also present in the amino-terminal domain (NTD) of the Omicron spike glycoprotein. The 69-70 deletion is also found in the Alpha and Eta (B.1.525) variants and is associated with enhanced fusogenicity and incorporation of cleaved spike into virions[10] . This deletion can also be used as a useful proxy for prevalence estimates in the population by S-gene target failure (SGTF) using the TaqPath™ (Applied Biosystems, Pleasanton, CA) diagnostic assay. Deletions in the vicinity of amino acids 143-145 have been shown to affect a range of NTD-specific neutralising antibodies[11,12] . Two mutations (N679K and P681H) at the S1/S2 furin cleavage site (FCS), have individually been found to enhance furin cleavage in other variants, contributing to enhanced infectivity, while a third (H655Y, also present in the Gamma VOC) occurs in the vicinity of the FCS[13]. The role of these changes in combination requires further investigation. Several mutations, such as the deletion at site 211, are not present at high frequency in other VOCs in the global sequencing data, suggesting historic negative selection[14]. Outside the spike protein, 15 amino acid substitutions are present and require further characterisation. For example, a deletion within NSP6 (105-107) may contribute to immune evasion through virus-induced cellular autophagy[15].

Critically, emerging data indicate that the Omicron variant evades neutralisation by sera obtained from people vaccinated with 1 or 2 doses of vaccine, especially when antibody titres are waning. Indicative studies have shown that 3 doses of Wuhan-strain based vaccines may provide only partial protection from infection with this variant, including unpublished data made available as a press release from Pfizer. Immune evasion by Omicron may have contributed to the extremely high transmission rates in countries with high vaccination rates or natural immunity (R_0 of 3-5 in the UK)[9,16–25].

In this study, we aimed to investigate the antigenic and biological properties of the Omicron variant that might underly immune evasion and increased transmission of the virus. We demonstrate that vaccine effectiveness is significantly reduced against the Omicron variant in association with neutralising antibody responses from dual and triple recipients of the BNT162b2 (Pfizer), ChAdOx1 (Astra Zeneca) and mRNA-1273 (Moderna) COVID-19 vaccines. Further, using live virus culture and viral pseudotypes, we describe an altered entry pathway that favours endosomal fusion over the TMPRSS2-dependent, cell surface fusion utilised by all previous variants of SARS-CoV-2. In summary, Omicron exhibits significant antigenic and biological changes that underpin immune evasion and hyper-transmissibility and could affect the pathogenesis and clinical severity of disease.

medRxiv preprint doi: https://doi.org/10.1101/2022.01.03.21268111; this version posted January 3, 2022. The copyright holder for this preprint (which was not certified by peer review) is the author/funder, who has granted medRxiv a license to display the preprint in perpetuity.
It is made available under a CC-BY-NC-ND 4.0 International license .

Results

The Omicron variant of SARS-CoV-2 displays substantial change within spike predicted to affect antigenicity and furin cleavage

The Omicron variant is characterised by significant changes within the RBD of the spike glycoprotein, regions targeted by class 1,2 and 3 RBD-directed antibodies, and within the NTD supersite (**Fig.1A**). Deep mutational scanning (DMS) estimates at mutated sites are predictive of substantially reduced monoclonal and polyclonal antibody binding and altered binding to human ACE2 (**Fig.1B**)[26]. Fourteen mutations (K417N, G446S, E484A, Q493R, G496S, Q498R and to a lesser extent, G339D, S371L, S373P, N440K, S477N, T478K, N501Y and Y505H) may be predicted to evade antibody binding based on a calculated escape fraction (a quantitative measure of the extent to which a mutation reduces polyclonal antibody binding by DMS). Seven Omicron RBD mutations (K417N, G446S, E484A, Q493R, G496S, Q498R and N501Y) have been shown previously to be associated with decreased antibody binding, importantly falling in epitopes corresponding to three major classes of RBD-specific neutralising antibodies. The mutations present in spike also involve key structural epitopes targeted by several monoclonal antibodies in current clinical use. Of these, seven bind to the RBM (bamlanivimab, cilgavimab, casirivimab, etesevimab, imdevimab, regdanvimab and tixagevimab) and neutralisation of Omicron has been shown to be negligible or absent. An eighth mAb, sotrovimab, targets a conserved epitope common to SARS-CoV-1 and SARS-CoV-2 outside the RBM and has only a small reduction (x3) in neutralisation potency[27–29]. Two mutations at the furin cleavage site (N679K and P681H) are individually predicted to increase furin cleavage, although the combination of these changes and an adjacent change with unknown function (H655Y, also present in the Gamma VOC) is unknown.

Emergence of the Omicron variant in the UK

Despite high vaccination rates and levels of natural immunity following previous exposure in the UK, the Omicron variant has rapidly become dominant. The evolutionary relationships of SARS-CoV-2 variants at a global level are shown in **Fig.1C**. The first 8 cases of Omicron were detected in the UK on the 27th and 28th November 2021 (2 in England and 6 in Scotland). Due to the rapid spread of Omicron, early genome sequences were highly related with an average genetic divergence between 1 and 7 single nucleotide polymorphisms (SNPs) (**Fig.1D**). The phylogenetic relationship to Omicron sequences from other countries was consistent with multiple introductions associated with travel to South Africa followed by community transmission (discussed further in **Supplementary Information**). Within Scotland, 111 cases were detected in the first 10 days of the outbreak, spread across 9 separate Health Boards, the majority in NHS Greater Glasgow & Clyde (NHS GG&C).

medRxiv preprint doi: https://doi.org/10.1101/2022.01.03.21268111; this version posted January 3, 2022. The copyright holder for this preprint **(which was not certified by peer review)** is the author/funder, who has granted medRxiv a license to display the preprint in perpetuity.
It is made available under a CC-BY-NC-ND 4.0 International license .

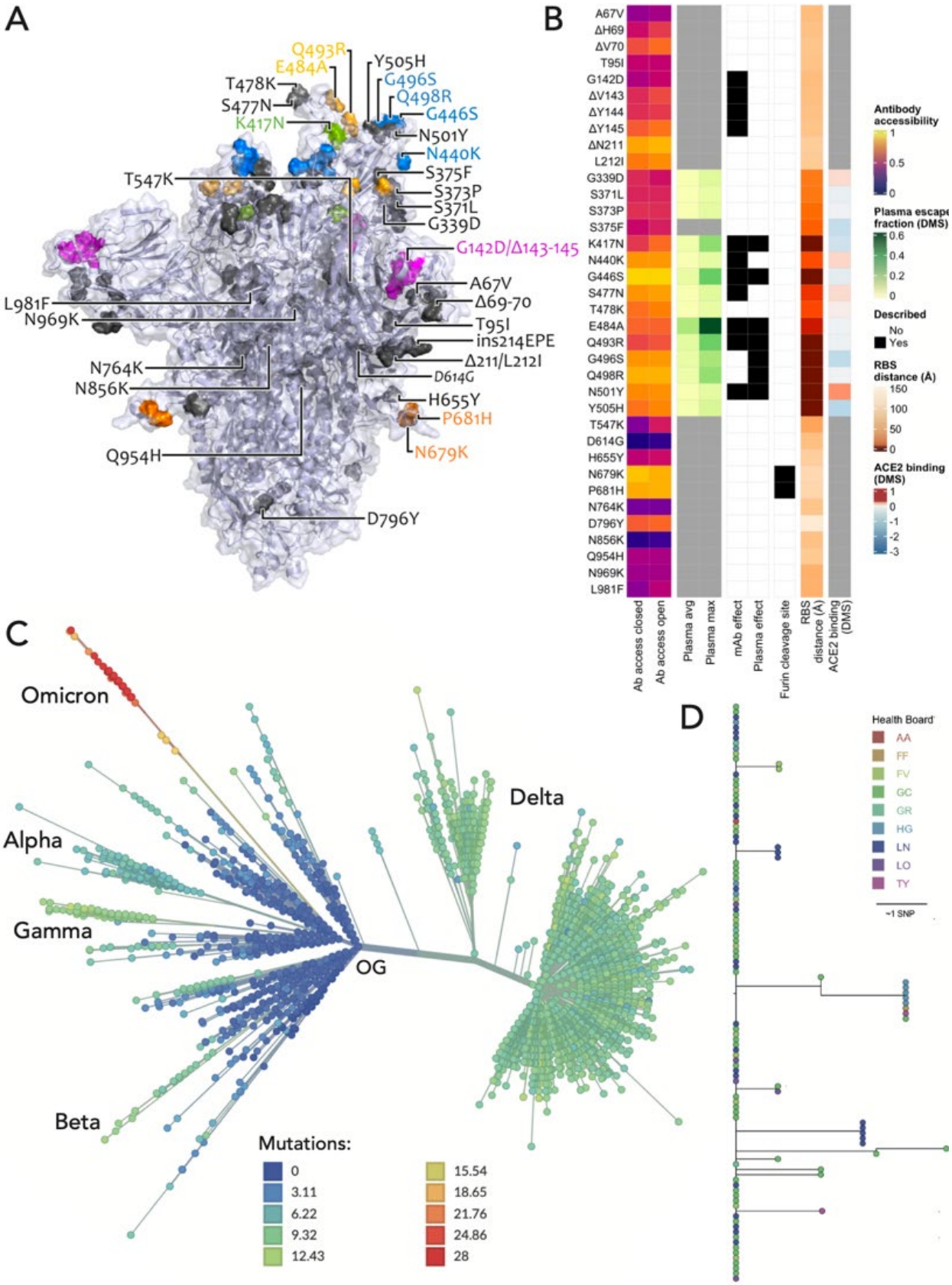

medRxiv preprint doi: https://doi.org/10.1101/2022.01.03.21268111; this version posted January 3, 2022. The copyright holder for this preprint (which was not certified by peer review) is the author/funder, who has granted medRxiv a license to display the preprint in perpetuity.
It is made available under a CC-BY-NC-ND 4.0 International license .

Figure 1 - Spike amino acid changes typifying the Omicron variant. (A) Spike homotrimer in open conformation with locations of Omicron amino acid substitutions, deletions (Δ), or insertions (ins) highlighted as spheres with opaque surface representation. Colouring highlights mutations at residues with substitutions impacting RBD-specific antibodies of classes 1 (green), 2 (yellow), and 3 (blue)[30] , or that belong to the NTD antibody supersite (magenta)[11], or that belong to the FCS (orange), with the remainder in grey. These are annotated on the monomer with an 'up' receptor-binding domain. The substitution D614G which is shared by common descent by all lineage B.1 descendants is italicised. The visualisation is made using a complete spike model[31] which is in turn based upon a partial cryo-EM structure (RCSB Protein Data Bank (PDB) ID: 6VSB[32]). (B) Aligned heatmaps showing properties of amino acid residues or of the specific amino acid substitution present in the Omicron variant, as appropriate (insertion not shown). Structure-based epitope scores[33] for residues in the structure of the original genotype spike in closed and open conformations are shown. For RBD residues, the results of deep mutational scanning (DMS) studies show the escape fraction (that is, a quantitative measure of the extent to which a mutation reduced polyclonal antibody binding) for each mutant averaged across plasma ('plasma average') and for the most sensitive plasma ('plasma max')[26]. Each mutation is classified as having evidence for mutations affecting neutralisation by either mAbs)[11,12,34–36] or antibodies in convalescent plasma from previously infected or vaccinated individuals[26,35–37]. Membership of the furin cleavage site is shown. The distance to ACE2-contacting residues that form the receptor-binding site (RBS) is shown (RBS defined as residues with an atom <4Å of an ACE2 atom in the structure of RBD bound to ACE2 (RCSB PDB ID: 6M0J [38]). Finally, ACE2 binding scores representing the binding constant (Δlog10 KD) relative to the wild-type reference amino acid from DMS experiments[39]. (**C**) Inferred evolutionary relationships of SARS-CoV-2 from NextStrain (https://nextstrain.org/ncov/gisaid/global) with the Variants of Concern labelled. The colours of the tree tips correspond to the number of mutations causing Spike amino acid substitutions relative to the SARS-CoV-2 original genotype (OG) reference strain Wuhan-Hu-1. (D) Inferred evolutionary relationships of the first 111 Omicron sequences in Scotland with NHS Scottish Health boards denoted: AA, Ayrshire and Arran; FF, Fife; FV, Forth Valley; GC, Great Glasgow and Clyde; GR, Grampian; HG, Highlands; LN, Lanarkshire; LO, Lothian; TY, Tayside, see key.

Neutralising responses to Omicron (BA.1) are substantially reduced following double and partially restored following triple vaccination

Levels of neutralising antibodies in patient sera correlate strongly with protection from infection[40–43], and reductions in neutralising activity against the Alpha and Delta variants are consistent with an observed reduction in vaccine effectiveness[2–5,44]. To investigate the likely effect of the mutations in the Omicron spike glycoprotein on vaccine effectiveness, sera collected from healthy volunteers at more than 14 days post-2nd dose vaccination with either BNT162b2, ChAdOx1 or mRNA-1273 were sorted into three age-matched groups (n=24 per group, mean age 45 years). Sera were first screened by electrochemiluminescence (MSD-ECL) assay for reactivity with SARS-CoV-2 antigens (Spike, RBD, NTD or nucleoprotein (N)). The antibody responses to RBD and NTD were significantly higher ($p<0.0001$) in the sera from individuals vaccinated with BNT162b2 or mRNA-1273 in comparison with the ChAdOx1 vaccinees (**Fig. 2A, Supp. Table S1**). In contrast, antibody responses to endemic human coronaviruses (HCoVs) (**Supp. Fig. S1, Supp. Table S2**) or influenza (**Supp. Fig. S2, Supp. Table S3**) were

medRxiv preprint doi: https://doi.org/10.1101/2022.01.03.21268111; this version posted January 3, 2022. The copyright holder for this preprint (which was not certified by peer review) is the author/funder, who has granted medRxiv a license to display the preprint in perpetuity.
It is made available under a CC-BY-NC-ND 4.0 International license .

similar, with the exception of coronavirus OC43, where responses in BNT162b2 and ChAdOx1 vaccinees differed significantly, perhaps suggesting modulation (back-boosting) of pre-existing OC43 responses by BNT162b2 vaccination.

Next, the neutralising antibody responses against SARS-CoV-2 pseudotypes expressing the spike glycoprotein from either Wuhan-Hu-1, or Omicron (BA.1) were compared (**Fig. 3B**). Vaccination with mRNA-1273 elicited the highest neutralising antibody titres (mean titre Wuhan=21,118, Omicron=285), in comparison with those elicited by vaccination with either BNT162b2 (Wuhan=4978, Omicron=148.3) or ChAdOx1 (Wuhan=882.3, Omicron=61.9). Neutralising antibody titres against Wuhan differed significantly between the three study groups. Activity against Omicron was markedly reduced in comparison with Wuhan, reduced by 33-fold for BNT162b2, 14-fold for ChAdOX1 and 74-fold for mRNA-1273 (**Supp. Table S4**). While the fold change in neutralisation was lowest in recipients of the ChAdOx1 vaccine and highest in recipients of the mRNA-1273 vaccine, absolute neutralisation values were highest in mRNA-1273 followed by BNT162b2 and ChAdOx1. Neutralisation was lowest in the ChAdOx1 group, however it is important to note that this was given to older patients during early vaccine rollout in the UK, especially to vulnerable patients in nursing homes and was not recommended in young adults less than 40 years.

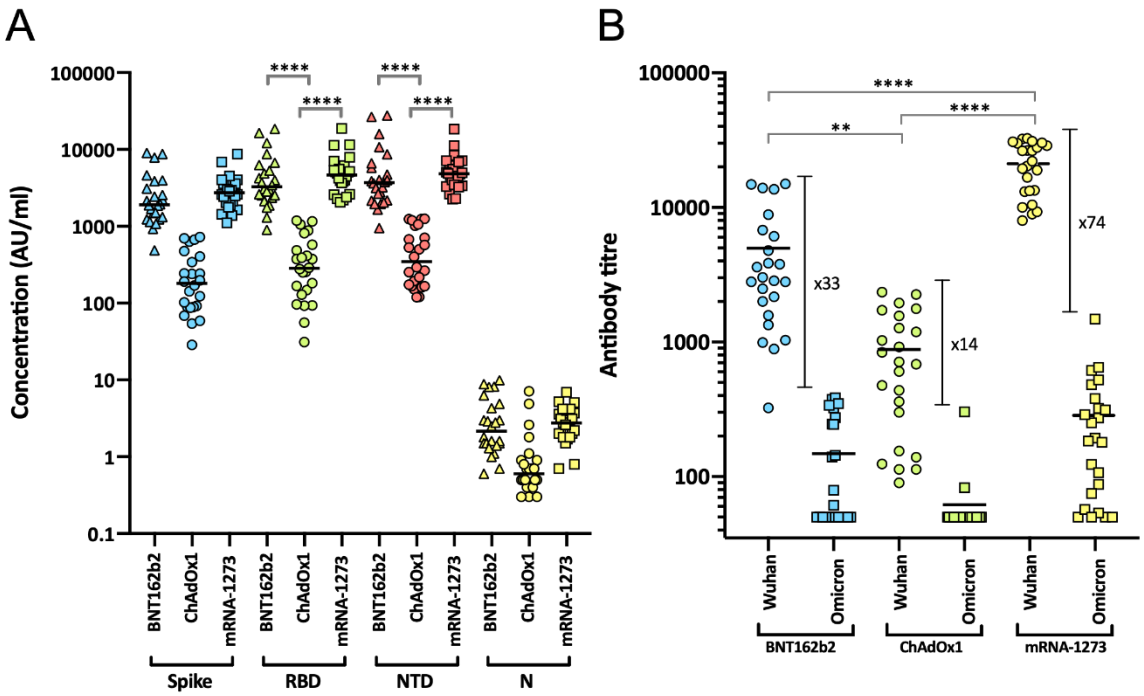

Figure 2 - Antibody responses elicited by two doses of SARS-CoV-2 vaccine. Antibody responses were studied in three groups of individuals (n=24 per group) vaccinated with either BNT162b2, ChAdOx1 or mRNA-1273 by (A) MSD-ECL assay or (B) pseudotype-based neutralisation assay. (A) Responses were measured against full-length spike glycoprotein (Spike), receptor binding domain (RBD), N-terminal domain (NTD) and nucleoprotein (N) and are expressed as arbitrary units (AU/ml).

medRxiv preprint doi: https://doi.org/10.1101/2022.01.03.21268111; this version posted January 3, 2022. The copyright holder for this preprint (which was not certified by peer review) is the author/funder, who has granted medRxiv a license to display the preprint in perpetuity.
It is made available under a CC-BY-NC-ND 4.0 International license .

(B) Neutralising antibody responses were quantified against Wuhan or Omicron spike glycoprotein bearing HIV(SARS-CoV-2) pseudotypes. Each point represents the mean of three replicates, bar represents the group mean. In panel B, % neutralising refers to the % of serum samples that displayed neutralising activity.

Next, samples were analysed from vaccine recipients at least 14 days post booster vaccination (third dose). Participants had been primed with two doses of either ChAdOx1 or BNT162b2, followed by a third dose of either BNT162b2 or mRNA-1273 (half dose; 50µg). All sera reacted strongly with SARS-CoV-2 antigens by MSD-ECL, with no significant differences between the four groups (**Fig. 3A, Supp. Table S5**). Antibody responses to HCoVs (**Supp. Fig. S3**, **Supp. Table S6**) or influenza (**Supp. Fig. S4**, **Supp. Table S7**) were similar, with the exception of influenza Michigan H1, where responses in ChAdOx1-primed and BNT162b2 or mRNA-1273-boosted groups differed significantly, likely reflecting co-administration of influenza booster vaccines during the booster campaign. Two vaccine recipients boosted with BNT162b2 displayed weak reactivity with nucleocapsid (**Fig. 3A**), suggesting previously undetected exposure to SARS-CoV-2. Sera from vaccine recipients primed with BNT162b2 and boosted with either BNT162b2 or mRNA-1273 displayed similar titres of neutralising antibody against Wuhan to the samples collected post-dose 2 (**Fig. 3B**). In contrast, vaccination of individuals primed with ChAdOx1 with a booster dose of either BNT162b2 or mRNA-1273 resulted in a marked increase in antibody titre (9.3-fold increase) against Wuhan relative to the low titres after dose 2 (**Fig. 3B**, **Supp. Table S8**). The marked increase in antibody titre in ChAdOx1-primed individuals (**Supp. Fig. S5**) emphasises the importance of the third dose booster in this population. Indeed, following boost with either BNT162b2 or mRNA-1273, anti-Wuhan neutralising antibody titres in the ChAdOx1-primed group were not significantly different from those primed with BNT162b2 (**Supp. Table S8**). Neutralising antibody titres against Omicron were lower in both booster study groups and did not differ significantly in titre (**Supp. Table S8**). However, absolute numbers displaying measurable Omicron neutralising activity were higher in the ChAdOx1-primed group (13/21, 62%) compared with the BNT162p2 primed group (5/20, 25%) (**Fig. 3B**).

medRxiv preprint doi: https://doi.org/10.1101/2022.01.03.21268111; this version posted January 3, 2022. The copyright holder for this preprint (which was not certified by peer review) is the author/funder, who has granted medRxiv a license to display the preprint in perpetuity.
It is made available under a CC-BY-NC-ND 4.0 International license .

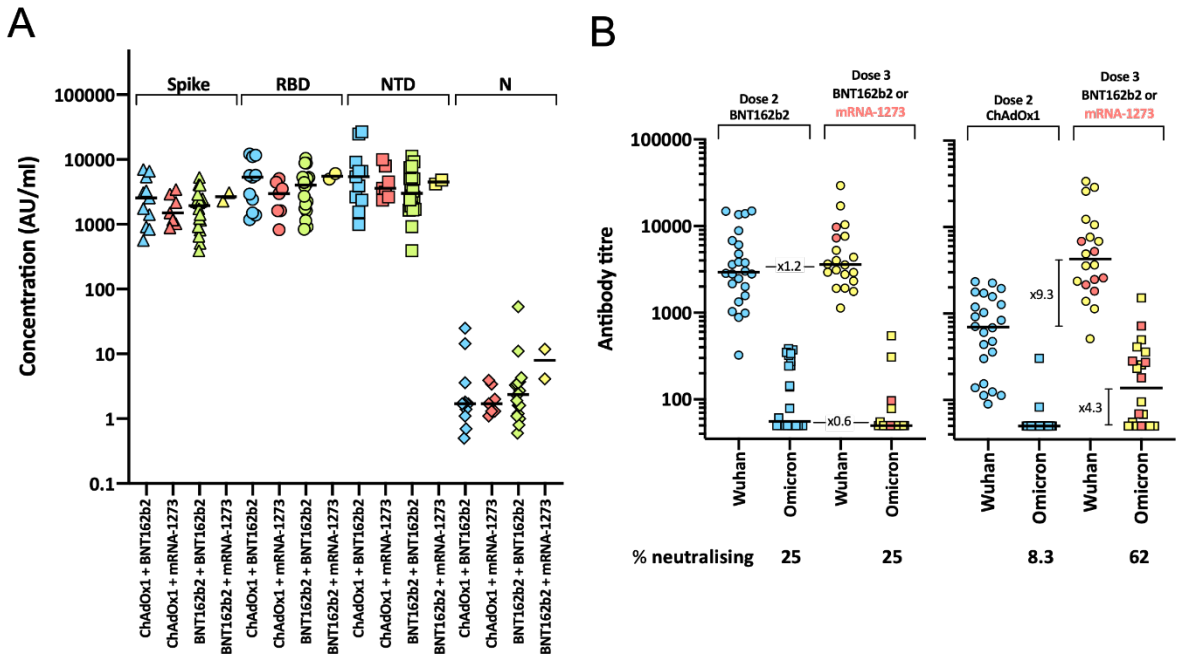

Figure 3 - Antibody responses elicited by SARS-CoV-2 booster vaccines. Antibody responses were studied in two groups of individuals primed with two doses of either BNT162b2 or ChAdOx1 and boosted with either BNT162b2 or mRNA-1273. Reactivity against SARS-CoV-2 antigens was measured by (A) MSD-ECL assay while neutralising activity (B) was measured using HIV (SARS-CoV-2) pseudotypes. (A) Responses were measured against full-length spike glycoprotein (Spike), receptor binding domain (RBD), N-terminal domain (NTD) and nucleoprotein (N) and are expressed as arbitrary units (AU/ml). (B) Neutralising antibody responses were quantified against Wuhan or Omicron spike glycoprotein-bearing HIV (SARS-CoV-2) pseudotypes. Each point represents the mean of three replicates, bar represents the group mean. Dose 3 sera from mRNA-1273 booster are in red, while those from BNT162b2 booster are in yellow. Fold changes between marked groups are indicated.

Vaccine effectiveness against infection with the Omicron variant is reduced compared to Delta

We next used a logistic additive model with a test negative case control design to estimate relative vaccine effectiveness against becoming a confirmed case with Delta (2553 cases) and/or Omicron (1001 cases) in a population of 1.2 million people in the largest health board in Scotland, NHS GG&C, between 6th -12th December 2021. Demographic data is shown in **Supp.Table S9** and **Supp.Fig.S6**. The timing of first doses of vaccination are shown in **Fig.4A** and the occurrence of sequenced/confirmed infections with different variants in vaccine recipients over time is shown in **Fig.4B**. Infection status for Omicron and Delta was modelled by number and product type of vaccine doses, previous infection status, sex, SIMD quartile, and age (to control for demographic bias). We ran two models, one with time since vaccination included, to estimate the protection provided by recent vaccination, and one without, to observe the current protection in today's mixed and waned population. Immunosuppressed individuals were removed from the analysis to ensure case-positivity could be

medRxiv preprint doi: https://doi.org/10.1101/2022.01.03.21268111; this version posted January 3, 2022. The copyright holder for this preprint (which was not certified by peer review) is the author/funder, who has granted medRxiv a license to display the preprint in perpetuity.
It is made available under a CC-BY-NC-ND 4.0 International license .

attributed to vaccine escape rather than an inability to mount a vaccine response. Age and time since vaccination were each modelled as single smooth effects using thin plate regression splines[45].

In both models, we estimated the protection from vaccine-acquired and infection-acquired immunity as being markedly reduced against Omicron compared with Delta. Estimates of vaccine effectiveness in recent recipients (at 14 days post-dose) were negative for full primary courses of ChAdOx1 against Omicron and only 16% against Delta. For two doses of mRNA vaccines, vaccine effectiveness was significantly lower for Omicron versus Delta; BNT162b2 (6.84% versus 56.53%) and mRNA-1273 (8.83% versus 60.07%) (**Fig.4C**). These responses increased significantly following a third booster dose of BNT162b2 or mRNA-1273 to 91.87% and 89.28% against Delta and 67.57% and 71.15% against Omicron. These estimates are similar to those reported against symptomatic infection recently in England where vaccine effectiveness was estimated as 71.4% and 75.5% for ChAdOx1 and BNT162b2 primary course recipients boosted with BNT162b2, respectively[18].

Our estimates of protection in the current GG&C cohort, whose median time since most recent dose is 5 months, were notably lower (**Fig.4D**). This waning of protection was evident for both variants, leading to very low levels of protection against Omicron in double vaccine recipients of ChAdOx1, BNT162b2 and mRNA-1273 (5.19%, 24.39% and 24.86% respectively). Our estimates for current protection against Omicron in recipients of a third booster dose of BNT162b2 or mRNA-1273 were much higher at 59.21% and 64.9%.

We next estimated the additive protective effect of previous natural infection. Infection-acquired immunity directed against other VOCs may be broader in nature and may wane more slowly than that induced by vaccines[46–48]. The level of protection following previous infection was 53.2% for Omicron, and 88.7% for Delta. This level of protection was greater than two doses of vaccine but did not reach levels attained by those who had never had natural infection and had received third dose boosters. These results collectively emphasise the importance of booster vaccines. The observation of waning protection indicates that in due course these may need to be repeated. Importantly, vaccine-mediated protection against severe disease is likely to be more durable than that against detected infection[49].

medRxiv preprint doi: https://doi.org/10.1101/2022.01.03.21268111; this version posted January 3, 2022. The copyright holder for this preprint (which was not certified by peer review) is the author/funder, who has granted medRxiv a license to display the preprint in perpetuity.
It is made available under a CC-BY-NC-ND 4.0 International license .

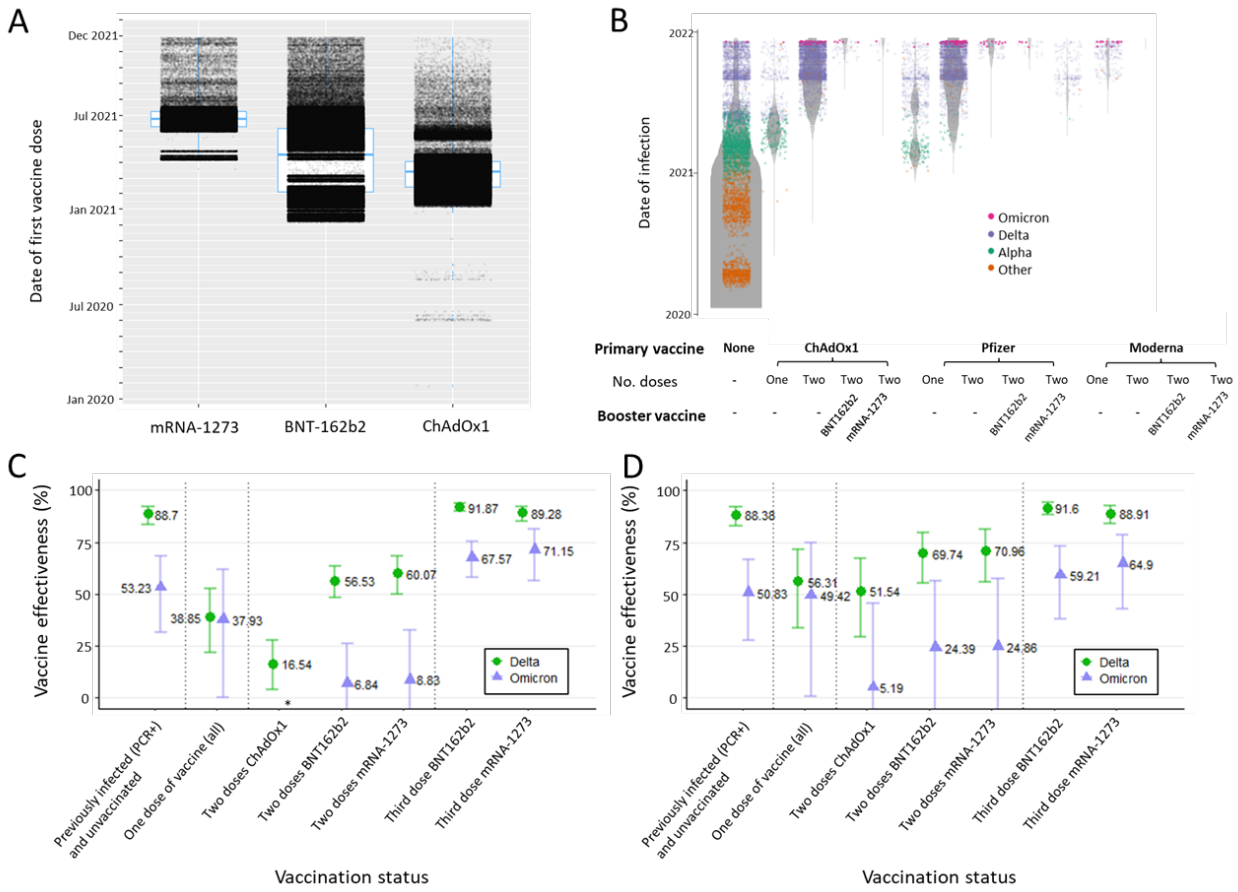

Figure 4 - Vaccine deployment and vaccine effectiveness estimates. (A) Date of first administered vaccine dose by vaccine product for the population of NHS Greater Glasgow and Clyde (NHS GG&C) aged 18 and older. **(B)** Denominator plot showing populations of test positive and test negative cohorts in NHS GG&C, with VOC classification of sequenced cases overlaid. The widths of the grey bands represent the populations in each group at each time point. **(C)** and **(D)** Estimated vaccine effectiveness against testing positive for Delta and Omicron SARS-CoV-2 infection in the population of over 18s in NHS GG&C who were tested between 6th and 12th December 2021, with the waning effect of vaccination over time excluded (C) and included (D). The additive effect of infection-acquired immunity was calculated for the entire population and plotted for the unvaccinated cohort. *The interval estimate for vaccine effectiveness against Omicron for two doses of ChAdOx1 was negative (CI: -74.2% to -16.1%) for the model without the waning effect of vaccination.

medRxiv preprint doi: https://doi.org/10.1101/2022.01.03.21268111; this version posted January 3, 2022. The copyright holder for this preprint (which was not certified by peer review) is the author/funder, who has granted medRxiv a license to display the preprint in perpetuity.
It is made available under a CC-BY-NC-ND 4.0 International license .

Isolation of SARS-CoV-2 Omicron from clinical samples.

We obtained nasopharyngeal swabs from 5 patients who were confirmed to be PCR-positive for infection with the SARS-CoV-2 Omicron variant. We attempted virus isolation in BHK-21 cells stably expressing the human ACE2 protein (BHK-hACE2) and VERO cells stably expressing ACE2 and TMPRSS2 (VAT[69]). The infected cells were incubated at 37°C and the cells monitored for signs of cytopathic effect (CPE) and the presence of viral progeny in the medium by RT-qPCR. While we observed no CPE in any of the infected cells, by RT-qPCR data at 5 days post-infection (dpi) we confirmed the presence of the virus derived from two of the five samples (referred from now on as 204 and 205) only in the medium of BHK-hACE2, but not VAT cells (**Supp.Fig. S7A**). An aliquot of the clarified medium containing approximately $4x10^4$ viral genomes of the P0 stocks of samples 204 and 205 was used to infect VAT, BHK-ACE2 and Calu-3 cells. Again, no CPE was observed in any of the infected cells but virus replication was confirmed in BHK-Ace2 and Calu-3 by RT-qPCR. Supernatants (termed P1) from infected Calu-3 cells at 3 dpi were collected and virus titrated by both focus forming assay and RT-qPCR. We found that the virus reached more than 100-fold higher titres in Calu-3 cells compared to BHK-hACE2 (**Supp.Fig. S7B**). Further passage of sample 205-derived P1 virus in both Calu-3 and Caco-2 yielded equivalent genome copy numbers in both cell lines (**Supp.Fig. S7B**). We observed CPE at 3 dpi in both Calu-3 and Caco2 cells (not shown). The medium (termed P2) of infected Calu-3 and Caco2 cells was collected at 4 dpi, titrated and used in the experiments described below.

Omicron does not induce cell syncytia

Our data demonstrate that antigenic change in Omicron permits evasion of vaccine induced immunity, however, the constellation of spike mutations in Omicron suggest that functional change may also contribute to its rapid transmission (**Fig.1A**). Therefore, we investigated the virological properties of live Omicron isolated from a patient sample. SARS-CoV-2 particles can achieve membrane fusion at the cell surface following proteolytic activation of spike by the plasma membrane protease TMPRSS2. This property also permits spike-mediated fusion of SARS-CoV-2 infected cells with adjacent cells resulting in syncytia[50]; this feature has been associated with severe disease[51]. The SARS-CoV-2 Delta variant has been shown to exhibit enhanced fusion compared to the Alpha and Beta variants[52]. We used the split GFP cell-cell fusion system[53] to quantify virus-induced cell fusion by Omicron, Delta and first wave Wuhan D614G virus (**Fig. 5A**). Cells expressing split GFP were infected with SARS-CoV-2 Wuhan-D614G, Delta or Omicron and the levels of the reconstituted GFP signal following cell-cell fusion was determined in real time (**Fig. 5B**). In addition, infected cells were probed by indirect immunofluorescence assay to assess viral replication by the detection of the viral nucleocapsid protein (**Fig. 5C**). The Delta variant exhibited the highest levels of cell fusion followed by Wuhan D614G.

medRxiv preprint doi: https://doi.org/10.1101/2022.01.03.21268111; this version posted January 3, 2022. The copyright holder for this preprint (which was not certified by peer review) is the author/funder, who has granted medRxiv a license to display the preprint in perpetuity.
It is made available under a CC-BY-NC-ND 4.0 International license .

Interestingly, the Omicron variant failed to promote fusion. This failure was not due to lack of infection as immunofluorescent detection of nucleocapsid protein confirmed viral replication by Omicron, as well as the other two variants. By immunofluorescence, syncytia were clearly evident in Wuhan D614G and Delta-infected cells, consistent with other recent reports[25].

Reduced replication kinetics of Omicron in lung epithelial cells

We next tested virus replication of Omicron, compared to Delta and Wuhan D614G in Calu-3, a human lung epithelial cell line. As shown in **Fig. 5D**, Wuhan D614G and Delta displayed comparable replication kinetics over a period of 72 hours, with visible CPE between 48-72hpi. The titres of the Omicron variant were instead at least an order of magnitude lower at each time point compared to the other two variants. This is consistent with attenuated replication of Omicron in lower respiratory tissues as recently reported[25,54].

medRxiv preprint doi: https://doi.org/10.1101/2022.01.03.21268111; this version posted January 3, 2022. The copyright holder for this preprint (which was not certified by peer review) is the author/funder, who has granted medRxiv a license to display the preprint in perpetuity.
It is made available under a CC-BY-NC-ND 4.0 International license .

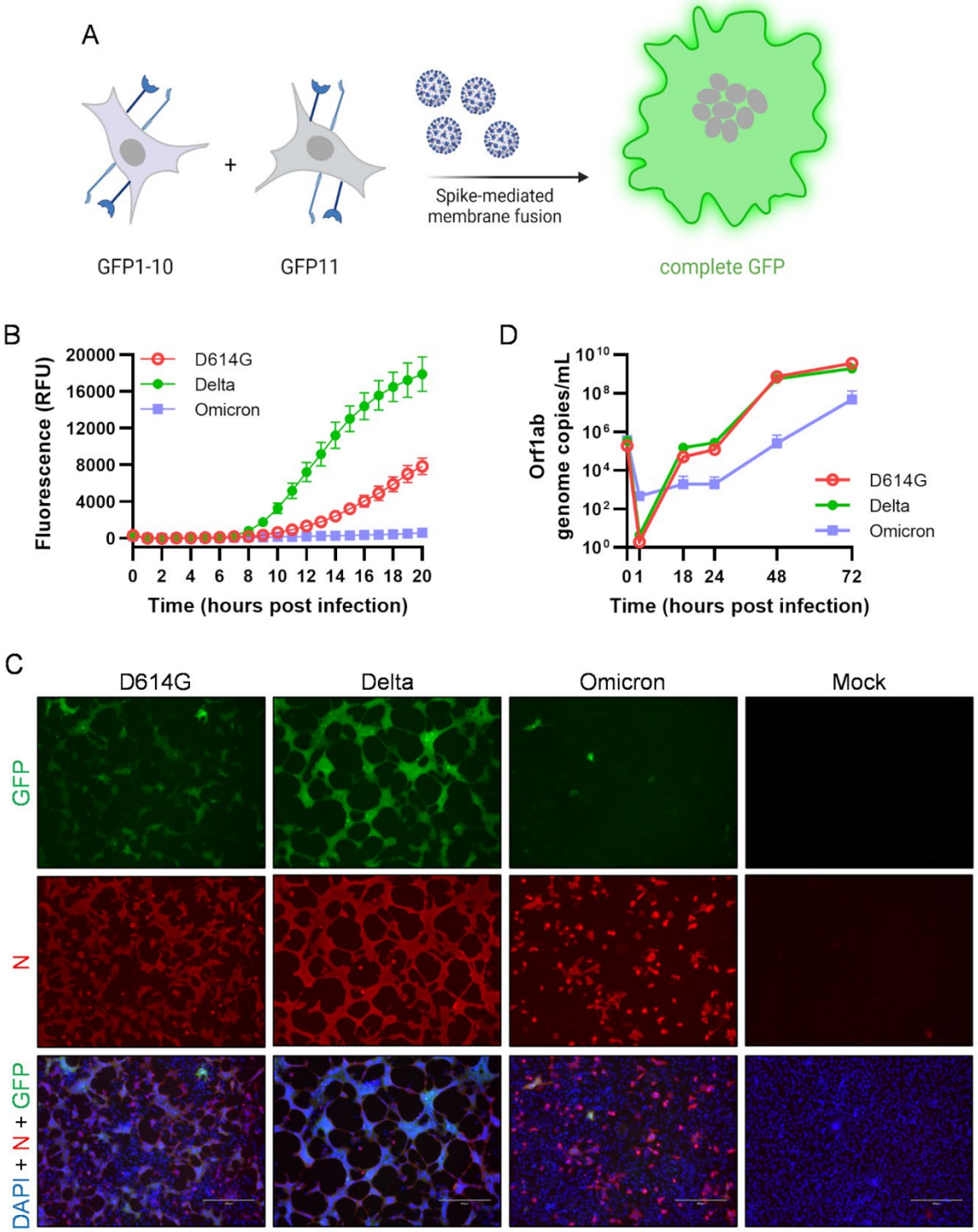

Figure 5. Reduced fusogenicity and replication kinetics by Omicron. A. Schematic representation of the split GFP system, used in this study to quantify virus induced cell fusion. This system is based on co-culture of two different cell lines (GFP-10 and GFP-11) expressing split GFP molecules. Upon virus-induced cell fusion, the intact GFP molecule is reconstituted and the resulting signal can be detected and quantified. **B.** GFP-10 and GFP-11 were co-cultured and infected with Wuhan D614G, Delta and Omicron and incubated in a CLARIOStar Plus (BMG LABTECH) at 37°C / 5% CO_2. GFP signal was measured every 30 min for 20h. Omicron infected cells showed only background levels of GFP signal. **C.** GFP-10 and GFP-11 infected cells were also analysed in parallel by immunofluorescence at 22h post-infection. Virus replication was assessed by detecting viral

medRxiv preprint doi: https://doi.org/10.1101/2022.01.03.21268111; this version posted January 3, 2022. The copyright holder for this preprint **(which was not certified by peer review)** is the author/funder, who has granted medRxiv a license to display the preprint in perpetuity.
It is made available under a CC-BY-NC-ND 4.0 International license .

nucleocapsid (N) expression using the appropriate antiserum and secondary antibodies. N expression can be detected in both Wuhan D614G, Delta and Omicron infected cells. However, syncytia can only be observed in Wuhan (D614G) and Delta infected cells. **D.** Replication kinetics of Wuhan D614G, Delta and Omicron. Calu-3 cells were infected with Wuhan D614G, Delta and Omicron and supernatants were collected at the indicated times and assessed by RT-qPCR. Omicron display reduced replication kinetics compared to Wuhan D614G and Omicron.

medRxiv preprint doi: https://doi.org/10.1101/2022.01.03.21268111; this version posted January 3, 2022. The copyright holder for this preprint (which was not certified by peer review) is the author/funder, who has granted medRxiv a license to display the preprint in perpetuity.
It is made available under a CC-BY-NC-ND 4.0 International license .

Omicron spike has switched entry route preference

Entry of SARS-CoV-2, and related coronaviruses, can proceed via two routes[55]. Cell surface fusion following proteolysis by TMPRSS2, as described above (Route 1; **Fig. 6A**), or fusion from the endosome after endocytosis and activation by the endosomal proteases Cathepsin B or L (Route 2; **Fig. 6A**). The ability of SARS-CoV-2 to achieve cell surface fusion is dependent on its S1/S2 polybasic cleavage site; this is absent from most closely related sarbecoviruses, which are confined to endosomal fusion[56–58]. Given the reduced fusogenicity and replication kinetics of Omicron, we used HIV pseudotypes to evaluate entry route preference. We evaluated Wuhan D614G, Alpha, Delta and Omicron spike and as a control we included Pangolin CoV (Guangdong isolate) spike, which exhibits high affinity interactions with human ACE2 but lacks a polybasic cleavage site and, therefore, enters via the endosome only[59–62].

Calu-3 cells predominantly support cell surface (Route 1) fusion, owing to their high endogenous expression of TMPRSS2[57,63]; in these cells, Delta yielded the highest infection, being ~4 fold higher than Omicron (**Fig. 6B**). Pangolin CoV infection was low, indicating that Calu-3 cells do not support robust endosomal entry. On the contrary, HEK only support endosomal entry and in these cells Pangolin CoV had high infection. Notably, Omicron also achieved high infection in HEK cells, producing ~10 fold greater signal than Delta. This suggests that Omicron, like Pangolin CoV, is optimised for endosomal entry. All pseudotypes exhibited robust infection in A549 ACE2 TMPRSS2, where both entry routes are available[64,65].

Entry pathway preference was further investigated using protease inhibitors targeting either TMPRSS2 (Camostat) or cathepsins (E64d)[58]. In Calu-3 cells, all SARS-CoV-2 pseudotypes were inhibited by Camostat, whereas only Omicron exhibited E64d sensitivity, indicating that a component of infection occurs via endosomal entry (**Fig. 6C**). In HEK cells all pseudotypes were inhibited by E64d, whereas Camostat was non-inhibitory; this confirms that only endosomal entry is available in these cells. Inhibitor treatment in A549 ACE2 TMPRSS2 provided the clearest evidence of altered entry by Omicron. D614G, Alpha and Delta were potently inhibited by Camostat, but not E64d. For Omicron, and Pangolin CoV, this pattern was completely reversed, suggesting a binary switch from cell surface to endosomal fusion; this conclusion was supported by titration of either inhibitor in A549 ACE2 TMPRSS2 cells (**Fig. 6D**).

These data indicate that, whilst Delta is optimised for fusion at the cell surface, Omicron preferentially achieves entry through endosomal fusion; this biological about-face may impact transmission, cellular tropism and pathogenesis. Moreover, this switch away from TMPRSS2-mediated activation offers a mechanistic explanation for reduced syncytia formation by Omicron infected cells.

medRxiv preprint doi: https://doi.org/10.1101/2022.01.03.21268111; this version posted January 3, 2022. The copyright holder for this preprint (which was not certified by peer review) is the author/funder, who has granted medRxiv a license to display the preprint in perpetuity.
It is made available under a CC-BY-NC-ND 4.0 International license .

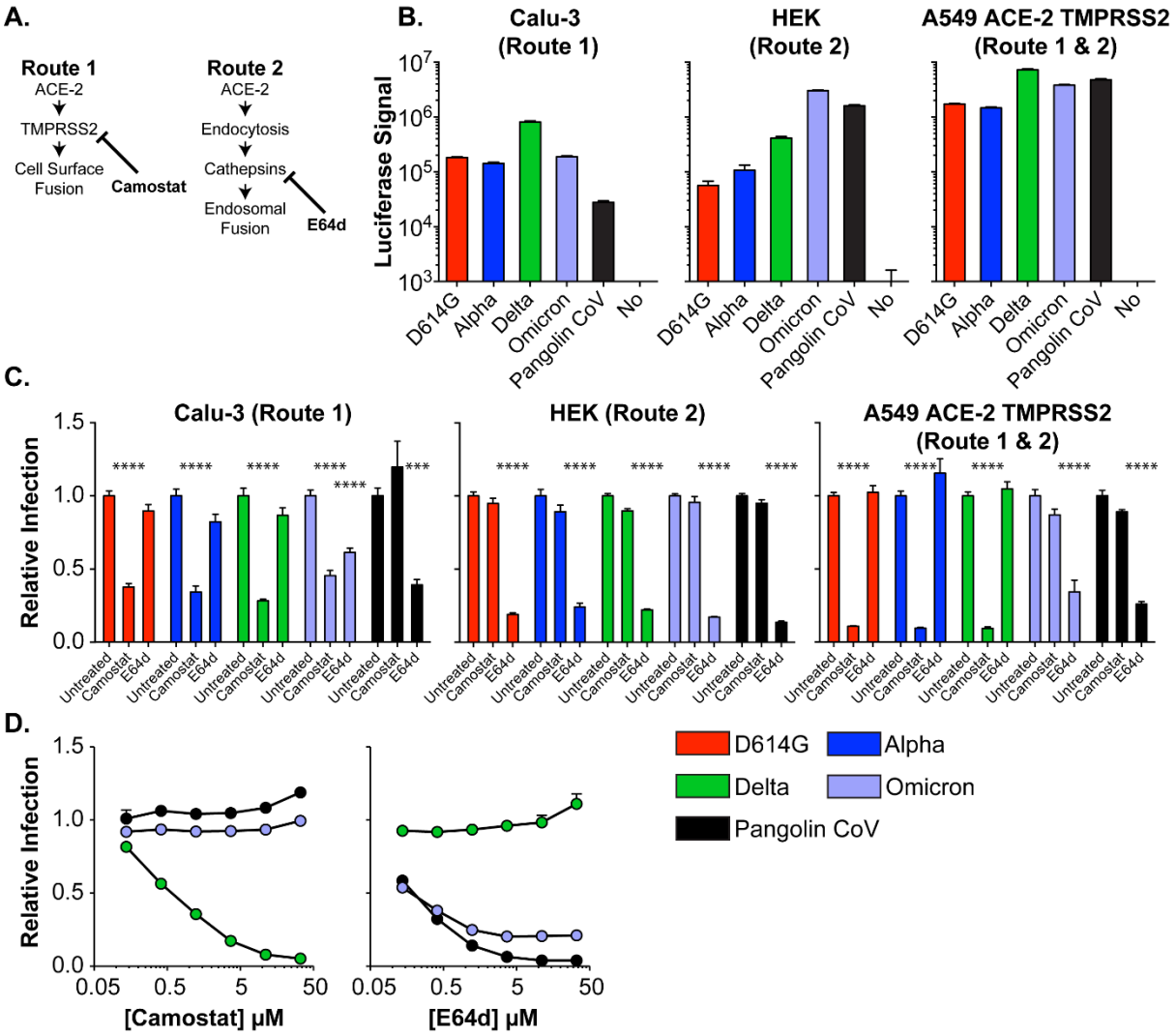

Figure 6. Omicron spike has switched entry route preference. A. SARS CoV-2 entry can occur via two routes. Route 1 permits rapid fusion at the cell surface following proteolytic processing by TMPRSS2. In Route 2 fusion occurs following endocytosis after processing by cathepsin B or L. Route 1 and 2 can be specifically inhibited using the protease inhibitors Camostat and E64d, respectively. **B.** SARS-CoV-2 pseudotype infection of the stated cell lines, data represent mean luciferase values from one representative experiment. In Calu-3 cells Route 1 entry predominates whereas HEK exclusively support Route 2, A549 ACE2 TMPRSS2 cells permit both routes. Pangolin CoV spike is included as a control; it can only achieve entry via Route 2. Pseudotypes without viral glycoproteins (No) are included as a negative control. **C.** Relative SARS-CoV-2 pseudotype infection (compared to untreated control) of cells treated with 10μM protease inhibitors. Data represent mean of four replicates, error bars indicate standard error of the mean, asterisks indicate statistical significance (ANOVA). **D.** Titration of Camostat and E64d against Delta, Omicron and Pangolin CoV in A549 ACE2 TMPRSS2 cells, data points represent mean relative infection, compared to untreated control.

medRxiv preprint doi: https://doi.org/10.1101/2022.01.03.21268111; this version posted January 3, 2022. The copyright holder for this preprint (which was not certified by peer review) is the author/funder, who has granted medRxiv a license to display the preprint in perpetuity.
It is made available under a CC-BY-NC-ND 4.0 International license .

Conclusions

The Omicron variant represents a major change in biological function and antigenicity of SARS-CoV-2 virus. In this study, we demonstrate substantial immune escape of this variant with clear evidence of vaccine failure in dual vaccinated individuals and partial restoration of immunity following a third booster dose of mRNA vaccine. In addition, we demonstrate a shift in the SARS-CoV-2 entry pathway from cell surface fusion, triggered by TMPRSS2, to cathepsin-dependent fusion within the endosome. This fundamental biological shift may affect the pathogenesis and severity of disease and requires further evaluation in population-based studies.

Using sera from double vaccine recipients, we found that Omicron is associated with a drop in neutralisation greater in magnitude than that reported in all other variants of concern (including Beta and Delta). Boosting enhanced neutralising responses to both Wu-Hu-1 and Omicron, particularly in recipients of ChAdOx1, but did not completely overcome the inherent immune escape properties of Omicron. Importantly, we did not assess the impact of vaccination on clinical severity of disease which is likely to be much higher than detection of infection. Protection against severe disease is longer lasting than prevention of infection. We also did not measure the impact of vaccination on T cell immunity which may be better preserved as only 14% of CD8+ and 28% of CD4+ epitopes are predicted to be affected by key Omicron mutations[17].

In order to evaluate the impact of reduced neutralisation responses in vaccine recipients, we next assessed vaccine effectiveness. The probability of infection with Omicron versus the preceding Delta variant was significantly higher in double vaccine recipients, in keeping with the neutralisation data. A third dose of mRNA vaccine substantially reduced the probability of infection but did not restore immunity fully.

The observation of a highly transmissible variant that is associated with escape from vaccine-induced immune responses means that over time, Omicron-specific vaccines would be required if disease severity was high, either directed at the general population or vulnerable groups. Early indications in young people are that Omicron is 40-70% less severe than Delta[66,67] – similar calculations in the most vulnerable part of the population over the age of 40 years are awaited.

Genotypic change in new variants have previously been shown to alter viral phenotype by modulating innate immune responses as well as evasion of the adaptive immune response[15,68]. Additionally, mutations can alter spike functionality to impact transmission and pathogenesis. For example, a polybasic insertion at the S1/S2 spike junction that facilitates cleavage of the spike glycoprotein by furin during virus assembly[13]. This may have provided a selective advantage in lung cells and primary

medRxiv preprint doi: https://doi.org/10.1101/2022.01.03.21268111; this version posted January 3, 2022. The copyright holder for this preprint (which was not certified by peer review) is the author/funder, who has granted medRxiv a license to display the preprint in perpetuity.
It is made available under a CC-BY-NC-ND 4.0 International license .

human airway epithelial cells for the original emergent SARS-CoV-2, and previous VOCs by permitting spike activation by the plasma membrane protease TMPRSS2, enabling rapid cell surface fusion[55]. In this study, we found that the Omicron variant has switched entry pathway to preferentially use endosomal fusion that is independent of TMPRSS2; a major change in the biological behaviour of the virus. This switching in the mechanism of fusion activation also manifests in reduced syncytia formation in infected cells, likely to reduce the cell-to-cell transmission characteristic of other variants. These properties have the potential to substantially change cellular tropism and pathogenesis of disease. Nonetheless, even a variant that is less virulent with a very high transmission rate may still present a substantial risk to older people and those with co-morbidities, especially those with immunosuppression. Moreover, our work demonstrates that SARS-CoV-2 exhibits high antigenic and functional plasticity; further fundamental shifts in transmission and disease should be anticipated.

Methods

Cells. Calu-3 are human lung adenocarcinoma epithelial cells. Caco-2 are an immortalized cell line derived from human colorectal adenocarcinoma, primarily used as a model of the intestinal epithelial barrier. A549 cells, a human alveolar adenocarcinoma line, were modified to stably express human ACE-2 and TMPRSS2. Human embryonic kidney (HEK293T) cells were used in pseudotype production. Baby Hamster Kidney clone 21 cells and Vero ACE-2 TMPRSS2 cells were used in the isolation of live Omicron SARS-CoV-2. All cell lines were maintained at 37°C and 5% CO_2 in DMEM supplemented with 10% foetal bovine serum (FBS), except for Calu-3 cells which were supplemented with 20% FBS.

Generation of cell line expressing human ACE2 receptor. Lentiviral vectors encoding human *ACE2* (GenBank NM_001371415.1) were produced as described previously[69] and BHK-21 transduced cells were selected with 200µg/ml of hygromycin B.

Generation of cell lines used for fusion assays. Retrovirus vectors were produced by transfecting HEK-293T cells with plasmid pQCXIP-GFP1-10 (Addgene #68715) or pQCXIP-BSR-GFP11 (Addgene #68716)[53] and packaging vectors expressing MLV gal-pol and VSV-G using Lipofectamine 3000 (Invitrogen) according to manufacturer's instructions. Cell supernatants were harvested 24-48h post-transfection, pooled, clarified by centrifugation and filtered. One mL of each supernatant was used to transduce A549-Ace2-TMPRSS2 (AAT) cells[69] in presence of Polybrene (Merck). Two days post-transduction, the supernatant was replaced with selection medium (DMEM 10% FBS 1µg/mL puromycin) and cells incubated until complete death of the untrasduced control cells were observed. The resulting puromycin-resistant cells (termed AAT-GFP1-10 and AAT-BSR-GFP11) were used in fusion assays.

medRxiv preprint doi: https://doi.org/10.1101/2022.01.03.21268111; this version posted January 3, 2022. The copyright holder for this preprint (which was not certified by peer review) is the author/funder, who has granted medRxiv a license to display the preprint in perpetuity.
It is made available under a CC-BY-NC-ND 4.0 International license .

Virus isolation from clinical sample. Nasopharyngeal swabs of patients infected with Omicron were collected with biorepository ethical approval (reference 10/S1402/33) in virus transport medium and resuspended in serum-free DMEM supplemented with 10 µg/ml gentamicin, 100 units/ml penicillin-streptomycin and 2.5µg/ml amphotericin B to a final volume of 1.5ml. BHK-hACE2 cells previously seeded at a cell density of 3x10^5 cells in T25 flask were inoculated with 400-500µL of resuspended samples in 5ml of complete medium (DMEM 2% FCS supplemented with gentamicin, penicillin-streptomycin and amphotericin B as above). After 20 hours, medium was replaced with fresh complete medium. Virus replication was monitored and confirmed over time by RT-qPCR since no clear cytopathic effect was observed. Culture supernatants (defined as P0) were harvested at day 4 post-infection. The P0 supernatant was next passaged in Calu-3 cells and after 3-4 days post-infection supernatant (P1) was harvested and stored at -80°C after clarification (500g x 10min) and used as working stock.

Measurement of SARS-CoV-2, HCoVs and influenza antibody response by electrochemiluminescence. IgG antibody titres were measured quantitatively against SARS-CoV-2 trimeric spike (S) protein, N-terminal domain (NTD), receptor binding domain (RBD) or nucleocapsid (N), human seasonal coronaviruses (HCoVs) 229E, OC43, NL63 and HKU1; and influenza A (Michigan H1, Hong Kong H3 and Shanghai H7) and B (Phuket HA and Brisbane) using MSD V-PLEX COVID-19 Coronavirus Panel 2 (K15369) and Respiratory Panel 1 (K15365) kits. Multiplex Meso Scale Discovery electrochemiluminescence (MSD-ECL) assays were performed according to manufacturer instructions. Briefly, 96-well plates were blocked for one hour. Plates were then washed, samples were diluted 1:5000 in diluent and added to the plates along with serially diluted reference standard (calibrator) and serology controls 1.1, 1.2 and 1.3. After incubation, plates were washed and SULFO-TAG detection antibody added. Plates were washed and were immediately read using a MESO Sector S 600 plate reader. Data were generated by Methodological Mind software and analysed using MSD Discovery Workbench (v4.0). Results are expressed as MSD arbitrary units per ml (AU/ml). Reference plasma samples yielded the following values: negative pool - spike 56.6 AU/ml, NTD 119.4 AU/ml, RBD 110.5 AU/ml and nucleocapsid 20.7 AU/ml; SARS-CoV-2 positive pool - spike 1331.1 AU/ml, NTD 1545.2 AU/ml, RBD 1156.4 AU/ml and nucleocapsid 1549.0 AU/ml; NIBSC 20/130 reference - spike 547.7 AU/ml, NTD 538.8 AU/ml, RBD 536.9 AU/ml and nucleocapsid 1840.2 AU/ml.

Measurement of virus neutralising antibodies using viral pseudotypes. Pseudotype-based neutralisation assays were carried out as described previously[2,69,70] . Briefly, HEK293, HEK293T, and 293-ACE2[69] cells were maintained in Dulbecco's modified Eagle's medium (DMEM) supplemented

medRxiv preprint doi: https://doi.org/10.1101/2022.01.03.21268111; this version posted January 3, 2022. The copyright holder for this preprint (which was not certified by peer review) is the author/funder, who has granted medRxiv a license to display the preprint in perpetuity.
It is made available under a CC-BY-NC-ND 4.0 International license .

with 10% FBS, 200mM L-glutamine, 100µg/ml streptomycin and 100 IU/ml penicillin. HEK293T cells were transfected with the appropriate SARS-CoV-2 S gene expression vector (wild type or variant) in conjunction with p8.91[71] and pCSFLW[72] using polyethylenimine (PEI, Polysciences, Warrington, USA). HIV (SARS-CoV-2) pseudotypes containing supernatants were harvested 48 hours post-transfection, aliquoted and frozen at -80°C prior to use. S gene constructs bearing the WUHAN (D614G) and Omicron (B.1.1.529) S genes were based on the codon-optimised spike sequence of SARS-CoV-2 and generated by GeneArt (ThermoFisher). Constructs bore the following mutations relative to the Wuhan-Hu-1 sequence (GenBank: MN908947): WUHAN(D614G) – D614G; Omicron (BA.1, B.1.1.529) - A67V, Δ69-70, T95I, G142D/Δ143-145, Δ211/L212I, ins214EPE, G339D, S371L, S373P, S375F, K417N, N440K, G446S, S477N, T478K, E484A, Q493R, G496S, Q498R, N501Y, Y505H, T547K, D614G, H655Y, N679K, P681H, N764K, D796Y, N856K, Q954H, N969K, L981F. 293-ACE2 target cells were maintained in complete DMEM supplemented with 2µg/ml puromycin.

Neutralising activity in each sample was measured by a serial dilution approach. Each sample was serially diluted in triplicate from 1:50 to 1:36450 in complete DMEM prior to incubation with HIV (SARS-CoV-2) pseudotypes, incubated for 1 hour, and plated onto 239-ACE2 target cells. After 48-72 hours, luciferase activity was quantified by the addition of Steadylite Plus chemiluminescence substrate and analysis on a Perkin Elmer EnSight multimode plate reader (Perkin Elmer, Beaconsfield, UK). Antibody titre was then estimated by interpolating the point at which infectivity had been reduced to 50% of the value for the no serum control samples.

Protease inhibitor studies. To selectively inhibit either cell surface or endosomal fusion of SARS-CoV-2, cells were pre-treated for one hour with 10µM of either Camostat mesylate (referred to hence forth as Camostat) or E64d prior to inoculation with pseudotype. In these studies, spike proteins from Alpha and Delta VOCs, and Guangdong isolate Pangolin coronavirus (GISAID ref EPI_ISL_410721) were used as controls.

Viral RNA extraction and RT-qPCR. Viral RNA was extracted from culture supernatants using the RNAdvance Blood kit (Beckman Coulter Life Sciences) following the manufacturer's recommendations. RNA was used as template to detect and quantify viral genomes by duplex RT-qPCR using a Luna® Universal Probe One-Step RT-qPCR Kit (New England Biolabs, E3006E). SARS-CoV-2 specific RNAs were detected by targeting the N1 gene from the CDC panel as part of the SARS-CoV-2 Research Use Only qPCR Probe Kit (Integrated DNA Technologies) and the ORF1ab gene using the following set of primers and probes: SARS-CoV-2_Orf1ab_Forward 5' GACATAGAAGTTACTGG&CGATAG 3', SARS-CoV-2_Orf1ab_Reverse 5' TTAATATGACGCGCACTACAG 3', SARS-CoV-2_Orf1ab_Probe ACCCCGTGACCTTGGTGCTTGT with HEX/ZEN/3IABkFQ modifications. SARS-CoV-2 RNA was used to

medRxiv preprint doi: https://doi.org/10.1101/2022.01.03.21268111; this version posted January 3, 2022. The copyright holder for this preprint (which was not certified by peer review) is the author/funder, who has granted medRxiv a license to display the preprint in perpetuity.
It is made available under a CC-BY-NC-ND 4.0 International license .

generate a standard curve and viral genomes were quantified and expressed as number of Orf1ab RNA molecules /ml of supernatant. All runs were performed on the ABI7500 Fast instrument and results analysed with the 7500 Software v2.3 (Applied Biosystems, Life Technologies).

Genome Sequencing and analysis. Sequencing was carried out by the UK public health agencies (UKHSA/PHE, PHS, PHW and PHNI) and by members of the COG-UK consortium using the ARTIC protocol as previously described.

Sequences were aligned by mapping to the SARS-CoV-2 reference Wuhan-Hu-1 using Minimap2 (https://doi.org/10.1093/bioinformatics/bty191). Prior to phylogenetic analysis 85 sites exhibiting high genetic variability due to data quality issues in overseas sequencing labs were excluded using a masking script in Phylopipe (https://github.com/cov-ert/phylopipe). The phylogenetic tree was constructed with the maximum likelihood method FastTree2 (https://doi.org/10.1371/journal.pone.0009490) using a JC+CAT nucleotide substitution model.

Replication curve. Calu-3 cells were seeded in a 96-well plate at a cell density of 3.5x10^4 cells per well. Cells were infected with the indicated viruses using the equivalent of 2x10^4 Orf1ab genome copies/well in serum-free RPMI-1640 medium (Gibco). After one hour of incubation at 37°C, cells were washed three times and left in 20% FBS RPMI-1640 medium. Supernatants were collected at different times post-infection and viral RNA extracted and quantified as described above.

Fusion assay. AAT-GFP1-10 and AAT-BSR-GFP11 cells were trypsinized and mixed at a ratio of 1:1 to seed a total of 2x10^4 cells/well in black 96-well plate (Greiner) in FluoroBrite DMEM medium (Thermo Fischer Scientific) supplemented with 2% FBS. Next day, cells were infected with the indicated viruses using the equivalent of 10^6 Orf1a genome copies/well in FluoroBrite DMEM 2% FBS. GFP signal was acquired for the following 20 hours using a CLARIOStar Plus (BMG LABTECH) equipped with ACU to maintain 37°C and 5% CO_2. Data were analysed using MARS software and plotted with GraphPad prims 9 software. At 22 hs post-infection, cells were fixed in 8% formaldehyde, permeabilized with 0.1 % Triton X-100 and stained with sheep anti-SARS-CoV-2 N (1:500) antiserum[73] followed by Alexa Fluor 594 Donkey anti-sheep IgG (H+L) (1:500, Invitrogen) and DAPI (1:4000, Sigma). Cell imagines were acquired using EVOS Cell Imaging Systems (Thermo Fischer Scientific).

Demographic data. Data for the EVADE study were available using the NHS Greater Glasgow and Clyde (NHS GG&C) SafeHaven platform and included vaccination status (dates and product names for each dose), demographic data (age, sex and Scottish Index of Multiple Deprivation (SIMD) quartile) comorbidity (shielding and immunosuppression status) and dates of positive and negative PCR tests, for 1.2 million inhabitants of the (NHS GG&C) area over 18 years of age, from 1st March 2020 up to

medRxiv preprint doi: https://doi.org/10.1101/2022.01.03.21268111; this version posted January 3, 2022. The copyright holder for this preprint (which was not certified by peer review) is the author/funder, who has granted medRxiv a license to display the preprint in perpetuity.
It is made available under a CC-BY-NC-ND 4.0 International license .

21st December 2021. Data were matched by CHI number and pseudonymised before analysis. Derogated ethical approval was granted by the NHS GG&C SafeHaven committee (GSH/21/IM/001).

Vaccine effectiveness. We used a logistic additive regression model to estimate relative vaccine effectiveness against the Omicron variant as it emerged in a population of 1.2 million people in NHS Greater Glasgow & Clyde, the largest health board in Scotland. Infection status for Omicron and Delta was modelled by number and product type of vaccine doses, previous infection status, sex, SIMD quartile, age on 31st October 2021 and time since most recent vaccination.

We identified Omicron infections using 3 data streams: confirmed S gene target failure (SGTF), allele specific PCR, and Pango lineage assignments from the sequencing data. SGTF samples with Delta lineage assignments were assigned as Delta infections. Samples for which the sequencing date was more than two weeks away from the first positive PCR were removed from the analysis.

We removed a small number of individuals who received ChAdOx1 as a third dose or had their third dose before the first of September 2021 on the assumption that the majority were part of the COV-BOOST clinical trial, the results of which are published elsewhere. We removed anyone with ambiguous vaccination status or whose brand was unknown due to data entry error.

Serum samples. Serum samples were collected from healthy participants in the COVID-19 Deployed Vaccine Cohort Study (DOVE), a cross-sectional post-licensing cohort study to determine the immunogenicity of deployed COVID-19 vaccines against evolving SARS-CoV-2 variants. 308 adult volunteers aged at least 18 years and were recruited into the study 14 days or more after a second or third dose of vaccine. All participants gave written informed consent to take part in the study. The DOVE study was approved by the North-West Liverpool Central Research Ethics Committee (REC reference 21/NW/0073).

Structural modelling. The file 6vsb_1_1_1.pdb containing a complete model of the full-length glycosylated spike homotrimer in open conformation with one monomer having the receptor-binding domain in the 'up' position was obtained from the CHARMM-GUI Archive [cite Woo et al. 2020, cite CHARMM-GUI 2021]. This model is itself generated based upon a partial spike cryo-EM structure (PDB ID: 6VSB). For visualisation, the model was trimmed to the ectodomain (residues 14-1164) and the signal peptide (residues 1-13) and glycans were removed. Using this structural model and the closed conformation equivalent (6vxx_1_1_1.pdb). Residues belonging to the receptor-binding site were identified as those with an atom within 4Å of an ACE2 atom in the bound RBD-ACE2 structure (PDB ID: 6M0J[38]) and Alpha carbon-to-Alpha carbon distances between these residues in the 'up' RBD and all

medRxiv preprint doi: https://doi.org/10.1101/2022.01.03.21268111; this version posted January 3, 2022. The copyright holder for this preprint (which was not certified by peer review) is the author/funder, who has granted medRxiv a license to display the preprint in perpetuity.
It is made available under a CC-BY-NC-ND 4.0 International license .

other spike residues were calculated. Antibody accessibility scores for open and closed conformations were calculated using BEpro[33]. Figures were prepared using PyMol[74].

Acknowledgments

The authors would like to thank the participants of the DOVE study and Sister Therese McSorley and her nursing team at the NHS GG&C clinical research facility. The authors also thank Alison Hamilton, Laura Stirling and Charlie Mayor from the NHS GG&C SafeHaven team for their invaluable input in facilitating this study. We thank Paula Olmo for administrative support and Chris Robertson and Aziz Sheikh for statistical advice. The authors thank all of the researchers who have shared genome data openly via the Global Initiative on Sharing All Influenza Data (GISAID).

Funding: The EVADE study is supported by HDR-UK (E.C.T). COG-UK is supported by funding from the Medical Research Council (MRC) part of UK Research & Innovation (UKRI), the National Institute of Health Research (NIHR) [grant code: MC_PC_19027], and Genome Research Limited, operating as the Wellcome Sanger Institute (G.M., R.M.B., D.L.R., E.C.T.). The COVID-19 DeplOyed VaccinE (DOVE) study is funded by the Medical Research Council core award (MCUU1201412) and COG-UK. We acknowledge the support of the G2P-UK National Virology Consortium (MR/W005611/1) funded by the UKRI (M.P.,E.C.T.). A.F., J.H., R.O and D.L.R acknowledge the MRC (MC_UU_12014/12) and DLR the Wellcome Trust (220977/Z/20/Z). W.T.H. is funded by the MRC (MR/R024758/1 and MR/W005611/1). N.L. and B.J.W. were funded by the Biotechnology and Biological Sciences Research Council (BBSRC, BB/R004250/1), G.T. was funded by the Department of Health and Social Care (DHSC, BB/R019843/1). J.G. is supported by a Sir Henry Dale Fellowship from the Wellcome Trust and Royal Society (107653/Z/15/A) and by the Medical Research Council (MC_UU_12014). The funders had no role in study design, data collection and analysis, decision to publish, or preparation of the manuscript.

References

1. WHO SPRP 2021 Mid-term Report - WHO Strategic Action Against COVID 19. https://www.who.int/publications/m/item/2021-mid-year-report---who-strategic-action-against-covid-19.

2. Davis, C. *et al.* Reduced neutralisation of the Delta (B. 1.617. 2) SARS-CoV-2 variant of concern following vaccination. *PLoS pathogens* **17**, e1010022 (2021).

3. Wall, E. C. *et al.* Neutralising antibody activity against SARS-CoV-2 VOCs B. 1.617. 2 and B. 1.351 by BNT162b2 vaccination. *The Lancet* **397**, 2331–2333 (2021).

medRxiv preprint doi: https://doi.org/10.1101/2022.01.03.21268111; this version posted January 3, 2022. The copyright holder for this preprint **(which was not certified by peer review)** is the author/funder, who has granted medRxiv a license to display the preprint in perpetuity.
It is made available under a CC-BY-NC-ND 4.0 International license .

4. Wall, E. C. *et al.* AZD1222-induced neutralising antibody activity against SARS-CoV-2 Delta VOC. *The Lancet* **398**, 207–209 (2021).

5. Lopez Bernal, J. *et al.* Effectiveness of Covid-19 vaccines against the B. 1.617. 2 (Delta) variant. *N Engl J Med* 585–594 (2021).

6. Viana, R. *et al.* Rapid epidemic expansion of the SARS-CoV-2 Omicron variant in southern Africa. *medRxiv* (2021).

7. Gu, H. *et al.* Probable Transmission of SARS-CoV-2 Omicron Variant in Quarantine Hotel, Hong Kong, China, November 2021. *Emerging infectious diseases* **28**, (2021).

8. Zahradník, J. *et al.* SARS-CoV-2 variant prediction and antiviral drug design are enabled by RBD in vitro evolution. *Nature microbiology* **6**, 1188–1198 (2021).

9. Cameroni, E. *et al.* Broadly neutralizing antibodies overcome SARS-CoV-2 Omicron antigenic shift. *bioRxiv* (2021).

10. Meng, B. *et al.* Recurrent emergence of SARS-CoV-2 spike deletion H69/V70 and its role in the Alpha variant B. 1.1. 7. *Cell reports* **35**, 109292 (2021).

11. McCallum, M. *et al.* N-terminal domain antigenic mapping reveals a site of vulnerability for SARS-CoV-2. *Cell* **184**, 2332–2347 (2021).

12. McCarthy, K. R. *et al.* Recurrent deletions in the SARS-CoV-2 spike glycoprotein drive antibody escape. *Science* **371**, 1139–1142 (2021).

13. Peacock, T. P. *et al.* The furin cleavage site in the SARS-CoV-2 spike protein is required for transmission in ferrets. *Nature Microbiology* 1–11 (2021).

14. Selection analysis identifies significant mutational changes in Omicron that are likely to influence both antibody neutralization and Spike function (Part 1 of 2) - SARS-CoV-2 coronavirus - Virological. https://virological.org/t/selection-analysis-identifies-significant-mutational-changes-in-omicron-that-are-likely-to-influence-both-antibody-neutralization-and-spike-function-part-1-of-2/771.

15. Benvenuto, D. *et al.* Evolutionary analysis of SARS-CoV-2: how mutation of Non-Structural Protein 6 (NSP6) could affect viral autophagy. *Journal of Infection* **81**, e24–e27 (2020).

16. Aggarwal, A. *et al.* SARS-CoV-2 Omicron: reduction of potent humoral responses and resistance to clinical immunotherapeutics relative to viral variants of concern. *medRxiv* (2021).

17. Ahmed, S. F., Quadeer, A. A. & McKay, M. SARS-CoV-2 T cell responses are expected to remain robust against Omicron. *bioRxiv* (2021).

18. Andrews, N. *et al.* Effectiveness of COVID-19 vaccines against the Omicron (B. 1.1. 529) variant of concern. *medRxiv* (2021).

19. Basile, K. *et al.* Improved neutralization of the SARS-CoV-2 Omicron variant after Pfizer-BioNTech BNT162b2 COVID-19 vaccine boosting. *bioRxiv* (2021).

20. Cao, Y. R. *et al.* B. 1.1. 529 escapes the majority of SARS-CoV-2 neutralizing antibodies of diverse epitopes. *BioRxiv* (2021).

medRxiv preprint doi: https://doi.org/10.1101/2022.01.03.21268111; this version posted January 3, 2022. The copyright holder for this preprint **(which was not certified by peer review)** is the author/funder, who has granted medRxiv a license to display the preprint in perpetuity.
It is made available under a CC-BY-NC-ND 4.0 International license .

21. Cele, S. *et al.* SARS-CoV-2 Omicron has extensive but incomplete escape of Pfizer BNT162b2 elicited neutralization and requires ACE2 for infection. *MedRxiv* (2021).

22. Dejnirattisai, W. *et al.* Reduced neutralisation of SARS-CoV-2 omicron B. 1.1. 529 variant by post-immunisation serum. *The Lancet* (2021).

23. Doria-Rose, N. *et al.* Booster of mRNA-1273 vaccine reduces SARS-CoV-2 Omicron escape from neutralizing antibodies. *medRxiv* (2021).

24. Garcia-Beltran, W. F. *et al.* mRNA-based COVID-19 vaccine boosters induce neutralizing immunity against SARS-CoV-2 Omicron variant. *Cell* (2021).

25. Meng, B. *et al.* SARS-CoV-2 Omicron spike mediated immune escape, infectivity and cell-cell fusion. *bioRxiv* (2021).

26. Greaney, A. J. *et al.* Comprehensive mapping of mutations in the SARS-CoV-2 receptor-binding domain that affect recognition by polyclonal human plasma antibodies. *Cell host & microbe* **29**, 463–476 (2021).

27. Burnett, D. L. *et al.* Immunizations with diverse sarbecovirus receptor-binding domains elicit SARS-CoV-2 neutralizing antibodies against a conserved site of vulnerability. *Immunity* **54**, 2908–2921 (2021).

28. Pinto, D. *et al.* Cross-neutralization of SARS-CoV-2 by a human monoclonal SARS-CoV antibody. *Nature* **583**, 290–295 (2020).

29. Rouet, R. *et al.* Potent SARS-CoV-2 binding and neutralization through maturation of iconic SARS-CoV-1 antibodies. in *Mabs* vol. 13 1922134 (Taylor & Francis, 2021).

30. Greaney, A. J. *et al.* Mapping mutations to the SARS-CoV-2 RBD that escape binding by different classes of antibodies. *Nature Communications 2021 12:1* **12**, 1–14 (2021).

31. Woo, H. *et al.* Developing a fully glycosylated full-length SARS-CoV-2 spike protein model in a viral membrane. *The Journal of Physical Chemistry B* **124**, 7128–7137 (2020).

32. Wrapp, D. *et al.* Cryo-EM structure of the 2019-nCoV spike in the prefusion conformation. *Science* **367**, 1260–1263 (2020).

33. Sweredoski, M. J. & Baldi, P. PEPITO: improved discontinuous B-cell epitope prediction using multiple distance thresholds and half sphere exposure. *Bioinformatics* **24**, 1459–1460 (2008).

34. Starr, T. N. *et al.* Prospective mapping of viral mutations that escape antibodies used to treat COVID-19. *Science* **371**, 850–854 (2021).

35. Weisblum, Y. *et al.* Escape from neutralizing antibodies by SARS-CoV-2 spike protein variants. *Elife* **9**, e61312 (2020).

36. Liu, Z. *et al.* Identification of SARS-CoV-2 spike mutations that attenuate monoclonal and serum antibody neutralization. *Cell host & microbe* **29**, 477–488 (2021).

37. Wang, Z. *et al.* mRNA vaccine-elicited antibodies to SARS-CoV-2 and circulating variants. *Nature* **592**, 616–622 (2021).

38. Lan, J. *et al.* Structure of the SARS-CoV-2 spike receptor-binding domain bound to the ACE2 receptor. *Nature* **581**, 215–220 (2020).

medRxiv preprint doi: https://doi.org/10.1101/2022.01.03.21268111; this version posted January 3, 2022. The copyright holder for this preprint **(which was not certified by peer review)** is the author/funder, who has granted medRxiv a license to display the preprint in perpetuity.
It is made available under a CC-BY-NC-ND 4.0 International license .

39. Starr, T. N. *et al.* Deep mutational scanning of SARS-CoV-2 receptor binding domain reveals constraints on folding and ACE2 binding. *Cell* **182**, 1295–1310 (2020).

40. Cromer, D. *et al.* Neutralising antibody titres as predictors of protection against SARS-CoV-2 variants and the impact of boosting: a meta-analysis. *The Lancet Microbe* (2021).

41. Gilbert, P. B. *et al.* Immune correlates analysis of the mRNA-1273 COVID-19 vaccine efficacy clinical trial. *Science* eab3435 (2021).

42. Earle, K. A. *et al.* Evidence for antibody as a protective correlate for COVID-19 vaccines. *Vaccine* (2021).

43. Khoury, D. S. *et al.* Neutralizing antibody levels are highly predictive of immune protection from symptomatic SARS-CoV-2 infection. *Nature medicine* 1–7 (2021).

44. Voysey, M. *et al.* Safety and efficacy of the ChAdOx1 nCoV-19 vaccine (AZD1222) against SARS-CoV-2: an interim analysis of four randomised controlled trials in Brazil, South Africa, and the UK. *The Lancet* **397**, 99–111 (2021).

45. Wood, S. N. *Generalized additive models: an introduction with R*. (chapman and hall/CRC, 2006).

46. Cho, A. *et al.* Anti-SARS-CoV-2 receptor-binding domain antibody evolution after mRNA vaccination. *Nature 2021 600:7889* **600**, 517–522 (2021).

47. Kim, P., Gordon, S. M., Sheehan, M. M. & Rothberg, M. B. Duration of SARS-CoV-2 Natural Immunity and Protection against the Delta Variant: A Retrospective Cohort Study. *Clinical Infectious Diseases* (2021) doi:10.1093/CID/CIAB999.

48. Goldberg, Y. *et al.* Protection and waning of natural and hybrid COVID-19 immunity. *medRxiv* 2021.12.04.21267114 (2021) doi:10.1101/2021.12.04.21267114.

49. Feikin, D. *et al.* Duration of Effectiveness of Vaccines Against SARS-CoV-2 Infection and COVID-19 Disease: Results of a Systematic Review and Meta-Regression. *SSRN Electronic Journal* (2021) doi:10.2139/SSRN.3961378.

50. Papa, G. *et al.* Furin cleavage of SARS-CoV-2 Spike promotes but is not essential for infection and cell-cell fusion. *PLoS pathogens* **17**, e1009246 (2021).

51. Braga, L. *et al.* Drugs that inhibit TMEM16 proteins block SARS-CoV-2 Spike-induced syncytia. *Nature* **594**, 88–93 (2021).

52. Zhang, J. *et al.* Membrane fusion and immune evasion by the spike protein of SARS-CoV-2 Delta variant. *Science* eabl9463 (2021).

53. Kodaka, M. *et al.* A new cell-based assay to evaluate myogenesis in mouse myoblast C2C12 cells. *Experimental cell research* **336**, 171–181 (2015).

54. Abdelnabi, R. *et al.* The omicron (B.1.1.529) SARS-CoV-2 variant of concern does not readily infect Syrian hamsters. *bioRxiv* 2021.12.24.474086 (2021) doi:10.1101/2021.12.24.474086.

55. Jackson, C. B., Farzan, M., Chen, B. & Choe, H. Mechanisms of SARS-CoV-2 entry into cells. *Nature Reviews Molecular Cell Biology* **23**, 3–20 (2022).

medRxiv preprint doi: https://doi.org/10.1101/2022.01.03.21268111; this version posted January 3, 2022. The copyright holder for this preprint **(which was not certified by peer review)** is the author/funder, who has granted medRxiv a license to display the preprint in perpetuity.
It is made available under a CC-BY-NC-ND 4.0 International license .

56. Hoffmann, M., Kleine-Weber, H. & Pöhlmann, S. A multibasic cleavage site in the spike protein of SARS-CoV-2 is essential for infection of human lung cells. *Molecular cell* **78**, 779–784 (2020).

57. Hoffmann, M. *et al.* SARS-CoV-2 cell entry depends on ACE2 and TMPRSS2 and is blocked by a clinically proven protease inhibitor. *cell* **181**, 271–280 (2020).

58. Mykytyn, A. Z. *et al.* SARS-CoV-2 entry into human airway organoids is serine protease-mediated and facilitated by the multibasic cleavage site. *Elife* **10**, e64508 (2021).

59. Nie, J. *et al.* Functional comparison of SARS-CoV-2 with closely related pangolin and bat coronaviruses. *Cell discovery* **7**, 1–12 (2021).

60. Wrobel, A. G. *et al.* Structure and binding properties of Pangolin-CoV spike glycoprotein inform the evolution of SARS-CoV-2. *Nature communications* **12**, 1–6 (2021).

61. Belouzard, S., Chu, V. C. & Whittaker, G. R. Activation of the SARS coronavirus spike protein via sequential proteolytic cleavage at two distinct sites. *Proceedings of the National Academy of Sciences* **106**, 5871–5876 (2009).

62. Dicken, S. J. *et al.* Characterisation of B. 1.1. 7 and Pangolin coronavirus spike provides insights on the evolutionary trajectory of SARS-CoV-2. *bioRxiv* (2021).

63. Saccon, E. *et al.* Cell-type-resolved quantitative proteomics map of interferon response against SARS-CoV-2. *Iscience* **24**, 102420 (2021).

64. Winstone, H. *et al.* The polybasic cleavage site in SARS-CoV-2 spike modulates viral sensitivity to type I interferon and IFITM2. *Journal of virology* **95**, e02422-20 (2021).

65. Daniloski, Z. *et al.* Identification of required host factors for SARS-CoV-2 infection in human cells. *Cell* **184**, 92–105 (2021).

66. Sheikh, A., Kerr, S., Woolhouse, M., McMenamin, J. & Robertson, C. Severity of omicron variant of concern and vaccine effectiveness against symptomatic disease: national cohort with nested test negative design study in Scotland. (2021).

67. Report 50 - Hospitalisation risk for Omicron cases in England | Faculty of Medicine | Imperial College London. https://www.imperial.ac.uk/mrc-global-infectious-disease-analysis/covid-19/report-50-severity-omicron/.

68. Thorne, L. G. *et al.* Evolution of enhanced innate immune evasion by SARS-CoV-2. *Nature* 1–12 (2021).

69. Hughes, E. C. *et al.* SARS-CoV-2 serosurveillance in a patient population reveals differences in virus exposure and antibody-mediated immunity according to host demography and healthcare setting. *Journal of Infectious Diseases* (2020).

70. Newman, J. *et al.* Neutralising antibody activity against SARS-CoV-2 variants, including Omicron, in an elderly cohort vaccinated with BNT162b2. *medRxiv* 2021.12.23.21268293 (2021) doi:10.1101/2021.12.23.21268293.

71. Zufferey, R., Nagy, D., Mandel, R. J., Naldini, L. & Trono, D. Multiply attenuated lentiviral vector achieves efficient gene delivery in vivo. *Nature biotechnology* **15**, 871–875 (1997).

medRxiv preprint doi: https://doi.org/10.1101/2022.01.03.21268111; this version posted January 3, 2022. The copyright holder for this preprint **(which was not certified by peer review)** is the author/funder, who has granted medRxiv a license to display the preprint in perpetuity.
It is made available under a CC-BY-NC-ND 4.0 International license .

72. Zufferey, R. *et al.* Self-Inactivating Lentivirus Vector for Safe and Efficient In Vivo Gene Delivery. *Journal of Virology* **72**, 9873–9880 (1998).

73. Rihn, S. J. *et al.* A plasmid DNA-launched SARS-CoV-2 reverse genetics system and coronavirus toolkit for COVID-19 research. *PLoS biology* **19**, e3001091 (2021).

74. Pymol, T. The PyMOL molecular graphics system. *Version* **1**, r3pre (2010).

medRxiv preprint doi: https://doi.org/10.1101/2022.01.03.21268111; this version posted January 3, 2022. The copyright holder for this preprint (which was not certified by peer review) is the author/funder, who has granted medRxiv a license to display the preprint in perpetuity.
It is made available under a CC-BY-NC-ND 4.0 International license .

Supplementary Information

Epidemiological description of the emergence of the Omicron variant in the UK

On the 27th November 2021, the UK Health Security Agency detected 2 cases of Omicron in England, the following day 6 Scottish cases were detected by community (Pillar 2) sequencing. Over the next 10 days (to 8th December 2021) a further 95 genome sequences were obtained. Due to the rapid spread of Omicron and low genetic diversity, the genome sequences are highly related with mean genetic divergence of 1 single nucleotide polymorphisms (SNPs) and maximum 7 SNPs.

The phylogenetic relationship to Omicron sequences from other countries is consistent with multiple introductions associated with travel to South Africa followed by community transmissions within Scotland. Amongst the Scottish samples diverged from the tree backbone, there were a number identified that are genetically divergent, i.e., greater than 2 single nucleotide polymorphisms from the nearest Scottish sample (Figure 1D). Moreover, comparison to the wider international collection of Omicron samples revealed that they were more closely related to genomes from other countries than other Scottish samples. These samples therefore likely represent independent introductions to Scotland, but without more detailed epidemiological data, the number of introductions is unknown. Where there are indistinguishable samples in the phylogeny from Scotland and elsewhere in world, importation cannot be ruled out as a source of these samples in Scotland, rather than transmission from an established population circulating in Scotland.

Within Scotland, cases are spread across 9 separate Health Boards and distributed throughout the phylogeny (Figure 1D). Basal Scottish genomes were sampled in 7 different Health Boards, most of them from NHS Greater Glasgow & Clyde (47%) and NHS Lanarkshire (25%). Notably, amongst these earliest samples are cases that were epidemiologically linked to early spreading events. All but one of these samples were found on this basal branch and are indistinguishable, and which is consistent with transmission at these events.

medRxiv preprint doi: https://doi.org/10.1101/2022.01.03.21268111; this version posted January 3, 2022. The copyright holder for this preprint (which was not certified by peer review) is the author/funder, who has granted medRxiv a license to display the preprint in perpetuity.
It is made available under a CC-BY-NC-ND 4.0 International license .

Supplementary Table S1. Comparison of SARS-CoV-2 antibody responses elicited by two doses of SARS-CoV-2 vaccine. Data were analyzed in GraphPad Prism v8.4.3, groups were compared by ordinary one-way ANOVA.

Tukey's multiple comparisons test	Mean Diff.	95.00% CI of diff.	Significant?	Summary	Adjusted P Value
Spike BNT162b2 vs. ChAdOx1	2588	-278.1 to 5453	No	ns	0.1212
Spike BNT162b2 vs. mRNA-1273	-248.4	-3114 to 2617	No	ns	>0.9999
Spike ChAdOx1 vs. mRNA-1273	-2836	-5702 to 29.73	No	ns	0.0553
RBD BNT162b2 vs. ChAdOx1	4649	1783 to 7514	Yes	****	<0.0001
RBD BNT162b2 vs. mRNA-1273	-449.1	-3315 to 2417	No	ns	>0.9999
RBD ChAdOx1 vs. mRNA-1273	-5098	-7964 to -2232	Yes	****	<0.0001
NTD BNT162b2 vs. ChAdOx1	5755	2889 to 8620	Yes	****	<0.0001
NTD BNT162b2 vs. mRNA-1273	714.7	-2151 to 3581	No	ns	0.9996
NTD ChAdOx1 vs. mRNA-1273	-5040	-7906 to -2174	Yes	****	<0.0001
N BNT162b2vs. ChAdOx1	2.183	-2864 to 2868	No	ns	>0.9999
N BNT162b2 vs. mRNA-1273	0.4	-2865 to 2866	No	ns	>0.9999
N ChAdOx1 vs. mRNA-1273	-1.783	-2868 to 2864	No	ns	>0.9999

medRxiv preprint doi: https://doi.org/10.1101/2022.01.03.21268111; this version posted January 3, 2022. The copyright holder for this preprint (which was not certified by peer review) is the author/funder, who has granted medRxiv a license to display the preprint in perpetuity.
It is made available under a CC-BY-NC-ND 4.0 International license .

Supplementary Table S2. Comparison of HCoV antibody responses elicited by two doses of SARS-CoV-2 vaccine. Data were analyzed in GraphPad Prism v8.4.3, groups were compared by ordinary one-way ANOVA.

Tukey's multiple comparisons test	Mean Diff.	95.00% CI of diff.	Significant?	Summary	Adjusted P Value
229E BNT162b2 vs. ChAdOx1	3296	-19673 to 26265	No	ns	>0.9999
229E BNT162b2 vs. mRNA-1273	5282	-17687 to 28251	No	ns	0.9998
229E ChAdOx1 vs. mRNA-1273	1986	-20982 to 24955	No	ns	>0.9999
OC43 BNT162b2 vs. ChAdOx1	39581	16612 to 62550	**Yes**	********	**<0.0001**
OC43 BNT162b2 vs. mRNA-1273	18396	-4573 to 41365	No	ns	0.2628
OC43 ChAdOx1 vs. mRNA-1273	-21185	-44154 to 1784	No	ns	0.1027
NL63 BNT162b2 vs. ChAdOx1	1317	-21652 to 24286	No	ns	>0.9999
NL63 BNT162b2 vs. mRNA-1273	696.9	-22272 to 23666	No	ns	>0.9999
NL63 ChAdOx1 vs. mRNA-1273	-620	-23589 to 22349	No	ns	>0.9999
HKU1 BNT162b2vs. ChAdOx1	17914	-5055 to 40883	No	ns	0.3015
HKU1 BNT162b2 vs. mRNA-1273	5468	-17501 to 28437	No	ns	0.9998
HKU1 ChAdOx1 vs. mRNA-1273	-12446	-35415 to 10523	No	ns	0.8243

medRxiv preprint doi: https://doi.org/10.1101/2022.01.03.21268111; this version posted January 3, 2022. The copyright holder for this preprint (which was not certified by peer review) is the author/funder, who has granted medRxiv a license to display the preprint in perpetuity.
It is made available under a CC-BY-NC-ND 4.0 International license .

Supplementary Table S3. Comparison of influenza antibody responses elicited by two doses of SARS-CoV-2 vaccine. Data were analyzed in GraphPad Prism v8.4.3, groups were compared by ordinary one-way ANOVA.

Tukey's multiple comparisons test	Mean Diff.	95.00% CI of diff.	Significant?	Summary	Adjusted P Value
Flu A Michigan H1 BNT162b2 vs. ChAdOx1	42355	-49090 to 133800	No	ns	0.9615
Flu A Michigan H1 BNT162b2 vs. mRNA-1273	34380	-57065 to 125825	No	ns	0.9943
Flu A Michigan H1 ChAdOx1 vs. mRNA-1273	-7975	-99420 to 83469	No	ns	>0.9999
Flu A Hong Kong H3 BNT162b2 vs. ChAdOx1	22853	-68592 to 114298	No	ns	>0.9999
Flu A Hong Kong H3 BNT162b2 vs. mRNA-1273	43959	-47486 to 135403	No	ns	0.948
Flu A Hong Kong H3 ChAdOx1 vs. mRNA-1273	21106	-70339 to 112550	No	ns	>0.9999
Flu A Shanghai H7 BNT162b2 vs. ChAdOx1	-3370	-94815 to 88074	No	ns	>0.9999
Flu A Shanghai H7 BNT162b2 vs. mRNA-1273	-5570	-97015 to 85874	No	ns	>0.9999
Flu A Shanghai H7 ChAdOx1 vs. mRNA-1273	-2200	-93645 to 89244	No	ns	>0.9999
Flu B Phuket HA BNT162b2 vs. ChAdOx1	54701	-36744 to 146145	No	ns	0.7707
Flu B Phuket HA BNT162b2 vs. mRNA-1273	83834	-7611 to 175279	No	ns	0.1132
Flu B Phuket HA ChAdOx1 vs. mRNA-1273	29133	-62311 to 120578	No	ns	0.999
Flu B Brisbane BNT162b2 vs. ChAdOx1	35122	-56323 to 126566	No	ns	0.993
Flu B Brisbane BNT162b2 vs. mRNA-1273	64342	-27102 to 155787	No	ns	0.5138
Flu B Brisbane ChAdOx1 vs. mRNA-1273	29220	-62224 to 120665	No	ns	0.999

medRxiv preprint doi: https://doi.org/10.1101/2022.01.03.21268111; this version posted January 3, 2022. The copyright holder for this preprint **(which was not certified by peer review)** is the author/funder, who has granted medRxiv a license to display the preprint in perpetuity.
It is made available under a CC-BY-NC-ND 4.0 International license .

Supplementary Table S4. Comparison of neutralising antibody titres elicited by two doses of SARS-CoV-2 vaccine. Neutralising antibody responses were quantified against Wuhan or Omicron spike glycoprotein-bearing HIV(SARS-CoV-2) pseudotypes. Data were analyzed in GraphPad Prism v8.4.3, groups were compared by ordinary one-way ANOVA.

Tukey's multiple comparisons test	Mean 1	Mean 2	Mean Diff.	95.00% CI of diff.	Significant?	Summary	Adjusted P Value
Wuhan BNT162b2 vs. ChAdOx1	4978	882.3	4096	733.8 to 7458	**Yes**	**	**0.0075**
Wuhan BNT162b2 vs. mRNA-1273	4978	21118	-16140	-19502 to -12778	**Yes**	****	**<0.0001**
Wuhan ChAdOx1 vs. mRNA-1273	882.3	21118	-20236	-23598 to -16874	**Yes**	****	**<0.0001**
Omicron BNT162b2 vs. ChAdOx1	148.3	61.9	86.39	-3276 to 3448	No	ns	>0.9999
Omicron BNT162b2 vs. mRNA-1273	148.3	285	-136.7	-3499 to 3225	No	ns	>0.9999
Omicron ChAdOx1 vs. mRNA-1273	61.9	285	-223.1	-3585 to 3139	No	ns	>0.9999
BNT162b2 Wuhan vs. Omicron	4978	148.3	4830	1468 to 8192	**Yes**	***	**0.0008**
ChAdOx12 Wuhan vs. Omicron	882.3	61.9	820.4	-2542 to 4182	No	ns	0.981
mRNA-1273 Wuhan vs. Omicron	21118	285	20833	17471 to 24195	**Yes**	****	**<0.0001**

medRxiv preprint doi: https://doi.org/10.1101/2022.01.03.21268111; this version posted January 3, 2022. The copyright holder for this preprint (which was not certified by peer review) is the author/funder, who has granted medRxiv a license to display the preprint in perpetuity.
It is made available under a CC-BY-NC-ND 4.0 International license .

Supplementary Table S5. Comparison of SARS-CoV-2 antibody responses elicited by a third dose of SARS-CoV-2 vaccine. Data were analyzed in GraphPad Prism v8.4.3, groups were compared by ordinary one-way ANOVA. P= BNT162b2, AZ = ChAdOx1, M = mRNA-1273.

Tukey's multiple comparisons test	Mean Diff.	95.00% CI of diff.	Significant?	Summary	Adjusted P Value
Spike AZ+P vs. AZ+M	1163	-4354 to 6680	No	ns	>0.9999
Spike AZ+P vs. P+P	1007	-3360 to 5374	No	ns	>0.9999
Spike AZ+P vs. P+M	361.3	-8410 to 9133	No	ns	>0.9999
Spike AZ+M vs. P+P	-156	-5239 to 4927	No	ns	>0.9999
Spike AZ+M vs. P+M	-801.5	-9951 to 8348	No	ns	>0.9999
Spike P+P vs. P+M	-645.5	-9151 to 7860	No	ns	>0.9999
RBD AZ+P vs. AZ+M	2675	-2842 to 8192	No	ns	0.9453
RBD AZ+P vs. P+P	1439	-2928 to 5806	No	ns	0.9988
RBD AZ+P vs. P+M	37.5	-8734 to 8809	No	ns	>0.9999
RBD AZ+M vs. P+P	-1236	-6319 to 3846	No	ns	>0.9999
RBD AZ+M vs. P+M	-2638	-11787 to 6511	No	ns	0.9997
RBD P+P vs. P+M	-1401	-9906 to 7104	No	ns	>0.9999
NTD AZ+P vs. AZ+M	3368	-2149 to 8885	No	ns	0.7418
NTD AZ+P vs. P+P	4098	-269.4 to 8465	No	ns	0.0919
NTD AZ+P vs. P+M	3739	-5033 to 12510	No	ns	0.9822
NTD AZ+M vs. P+P	729.8	-4353 to 5813	No	ns	>0.9999
NTD AZ+M vs. P+M	370.8	-8778 to 9520	No	ns	>0.9999
NTD P+P vs. P+M	-359	-8864 to 8146	No	ns	>0.9999
N AZ+P vs. AZ+M	2.755	-5514 to 5520	No	ns	>0.9999
N AZ+P vs. P+P	-0.7066	-4368 to 4366	No	ns	>0.9999
N AZ+P vs. P+M	-3.095	-8775 to 8768	No	ns	>0.9999
N AZ+M vs. P+P	-3.461	-5086 to 5079	No	ns	>0.9999
N AZ+M vs. P+M	-5.85	-9155 to 9143	No	ns	>0.9999
N P+P vs. P+M	-2.389	-8508 to 8503	No	ns	>0.9999

P = BNT162b2; AZ = ChAdOx1; M = mRNA-1273

medRxiv preprint doi: https://doi.org/10.1101/2022.01.03.21268111; this version posted January 3, 2022. The copyright holder for this preprint (which was not certified by peer review) is the author/funder, who has granted medRxiv a license to display the preprint in perpetuity.
It is made available under a CC-BY-NC-ND 4.0 International license .

Supplementary Table S6. Comparison of HCoV antibody responses elicited by a third dose of SARS-CoV-2 vaccine. Data were analyzed in GraphPad Prism v8.4.3, groups were compared by ordinary one-way ANOVA. P= BNT162b2, AZ = ChAdOx1, M = mRNA-1273.

Tukey's multiple comparisons test	Mean Diff.	95.00% CI of diff.	Significant?	Summary	Adjusted P Value
229E AZ+P vs. AZ+M	-11229	-47020 to 24562	No	ns	0.9993
229E AZ+P vs. P+P	-5670	-34000 to 22661	No	ns	>0.9999
229E AZ+P vs. P+M	4487	-52417 to 61391	No	ns	>0.9999
229E AZ+M vs. P+P	5560	-27414 to 38533	No	ns	>0.9999
229E AZ+M vs. P+M	15716	-43637 to 75069	No	ns	>0.9999
229E P+P vs. P+M	10156	-45019 to 65332	No	ns	>0.9999
OC43 AZ+P vs. AZ+M	-29568	-65359 to 6224	No	ns	0.2369
OC43 AZ+P vs. P+P	-121	-28451 to 28209	No	ns	>0.9999
OC43 AZ+P vs. P+M	-5301	-62205 to 51603	No	ns	>0.9999
OC43 AZ+M vs. P+P	29447	-3527 to 62420	No	ns	0.1382
OC43 AZ+M vs. P+M	24266	-35086 to 83619	No	ns	0.988
OC43 P+P vs. P+M	-5180	-60356 to 49996	No	ns	>0.9999
NL63 AZ+P vs. AZ+M	-11140	-46931 to 24651	No	ns	0.9994
NL63 AZ+P vs. P+P	-8074	-36404 to 20256	No	ns	0.9998
NL63 AZ+P vs. P+M	-16842	-73746 to 40062	No	ns	0.9996
NL63 AZ+M vs. P+P	3066	-29908 to 36040	No	ns	>0.9999
NL63 AZ+M vs. P+M	-5702	-65055 to 53651	No	ns	>0.9999
NL63 P+P vs. P+M	-8768	-63944 to 46407	No	ns	>0.9999
HKU1 AZ+P vs. AZ+M	9482	-26309 to 45273	No	ns	>0.9999
HKU1 AZ+P vs. P+P	8028	-20303 to 36358	No	ns	0.9998
HKU1 AZ+P vs. P+M	8678	-48226 to 65582	No	ns	>0.9999
HKU1 AZ+M vs. P+P	-1454	-34428 to 31519	No	ns	>0.9999
HKU1 AZ+M vs. P+M	-804.1	-60157 to 58549	No	ns	>0.9999
HKU1 P+P vs. P+M	650.4	-54525 to 55826	No	ns	>0.9999

P = BNT162b2; AZ = ChAdOx1; M = mRNA-1273

medRxiv preprint doi: https://doi.org/10.1101/2022.01.03.21268111; this version posted January 3, 2022. The copyright holder for this preprint (which was not certified by peer review) is the author/funder, who has granted medRxiv a license to display the preprint in perpetuity.
It is made available under a CC-BY-NC-ND 4.0 International license .

Supplementary Table S7. Comparison of influenza antibody responses elicited by a third dose of SARS-CoV-2 vaccine. Data were analyzed in GraphPad Prism v8.4.3, groups were compared by ordinary one-way ANOVA. P= BNT162b2, AZ = ChAdOx1, M = mRNA-1273.

Tukey's multiple comparisons test	Mean Diff.	95.00% CI of diff.	Significant?	Summary	Adjusted P Value
Flu A Michigan H1 AZ+P vs. AZ+M	410671	6882 to 814460	Yes	*	0.0413
Flu A Michigan H1 AZ+P vs. P+P	279008	-40609 to 598625	No	ns	0.1757
Flu A Michigan H1 AZ+P vs. P+M	459436	-182547 to 1101420	No	ns	0.5271
Flu A Michigan H1 AZ+M vs. P+P	-131663	-503667 to 240341	No	ns	0.9993
Flu A Michigan H1 AZ+M vs. P+M	48766	-620842 to 718373	No	ns	>0.9999
Flu A Michigan H1 P+P vs. P+M	180429	-442054 to 802911	No	ns	>0.9999
Flu A Hong Kong H3 AZ+P vs. AZ+M	-64025	-467814 to 339763	No	ns	>0.9999
Flu A Hong Kong H3 AZ+P vs. P+P	-32804	-352421 to 286812	No	ns	>0.9999
Flu A Hong Kong H3 AZ+P vs. P+M	56571	-585413 to 698554	No	ns	>0.9999
Flu A Hong Kong H3 AZ+M vs. P+P	31221	-340783 to 403225	No	ns	>0.9999
Flu A Hong Kong H3 AZ+M vs. P+M	120596	-549012 to 790204	No	ns	>0.9999
Flu A Hong Kong H3 P+P vs. P+M	89375	-533107 to 711857	No	ns	>0.9999
Flu A Shanghai H7 AZ+P vs. AZ+M	6841	-396948 to 410630	No	ns	>0.9999
Flu A Shanghai H7 AZ+P vs. P+P	469.8	-319147 to 320087	No	ns	>0.9999
Flu A Shanghai H7 AZ+P vs. P+M	9363	-632620 to 651346	No	ns	>0.9999
Flu A Shanghai H7 AZ+M vs. P+P	-6371	-378375 to 365633	No	ns	>0.9999
Flu A Shanghai H7 AZ+M vs. P+M	2522	-667086 to 672130	No	ns	>0.9999
Flu A Shanghai H7 P+P vs. P+M	8893	-613589 to 631376	No	ns	>0.9999
Flu B Phuket HA AZ+P vs. AZ+M	-101482	-505271 to 302307	No	ns	>0.9999
Flu B Phuket HA AZ+P vs. P+P	-6309	-325926 to 313308	No	ns	>0.9999
Flu B Phuket HA AZ+P vs. P+M	65660	-576323 to 707643	No	ns	>0.9999
Flu B Phuket HA AZ+M vs. P+P	95173	-276831 to 467178	No	ns	>0.9999
Flu B Phuket HA AZ+M vs. P+M	167142	-502466 to 836750	No	ns	>0.9999
Flu B Phuket HA P+P vs. P+M	71969	-550513 to 694451	No	ns	>0.9999
Flu B Brisbane AZ+P vs. AZ+M	-2954	-406743 to 400834	No	ns	>0.9999
Flu B Brisbane AZ+P vs. P+P	24661	-294956 to 344278	No	ns	>0.9999
Flu B Brisbane AZ+P vs. P+M	122461	-519522 to 764444	No	ns	>0.9999
Flu B Brisbane AZ+M vs. P+P	27615	-344389 to 399620	No	ns	>0.9999
Flu B Brisbane AZ+M vs. P+M	125415	-544193 to 795023	No	ns	>0.9999
Flu B Brisbane P+P vs. P+M	97800	-524683 to 720282	No	ns	>0.9999

P = BNT162b2; AZ = ChAdOx1; M = mRNA-1273

medRxiv preprint doi: https://doi.org/10.1101/2022.01.03.21268111; this version posted January 3, 2022. The copyright holder for this preprint (which was not certified by peer review) is the author/funder, who has granted medRxiv a license to display the preprint in perpetuity.
It is made available under a CC-BY-NC-ND 4.0 International license .

Supplementary Table S8. Effect of third dose of SARS-CoV-2 vaccine on neutralising antibody titres. Neutralising antibody responses were quantified against Wuhan or Omicron spike glycoprotein-bearing HIV (SARS-CoV-2) pseudotypes. Data were analyzed in GraphPad Prism v8.4.3, groups were compared by ordinary one-way ANOVA.

BNT162b2 prime (doses 1 & 2)					
Tukey's multiple comparisons test	**Mean Diff.**	**95.00% CI of diff.**	**Significant?**	**Summary**	**Adjusted P Value**
Wuhan (dose 2) vs. (dose 3)	-1186	-4381 to 2010	No	ns	0.7655
Omicron (dose 2) vs. (dose 3)	56.56	-3139 to 3252	No	ns	>0.9999
Test details	**Mean 1**	**Mean 2**	**Mean Diff.**	**SE of diff.**	**n1**
Wuhan (dose 2) vs. (dose 3)	4978	6164	-1186	1219	24
Omicron (dose 2) vs. (dose 3)	148.3	91.73	56.56	1219	24

ChAdOx1 prime (doses 1 & 2)					
Tukey's multiple comparisons test	**Mean Diff.**	**95.00% CI of diff.**	**Significant?**	**Summary**	**Adjusted P Value**
Wuhan (dose 2) vs. (dose 3)	-7360	-11073 to -3647	Yes	****	<0.0001
Omicron (dose 2) vs. (dose 3)	-203.7	-3916 to 3509	No	ns	0.9989
Test details	**Mean 1**	**Mean 2**	**Mean Diff.**	**SE of diff.**	**n1**
Wuhan (dose 2) vs. (dose 3)	882.3	8242	-7360	1416	24
Omicron (dose 2) vs. (dose 3)	61.9	265.5	-203.7	1416	24

Dose 3 titre comparison					
Tukey's multiple comparisons test	**Mean Diff.**	**95.00% CI of diff.**	**Significant?**	**Summary**	**Adjusted P Value**
Wuhan (BNT162b2 dose 2) vs. (ChAdOX1 dose 2)	-2079	-7008 to 2851	No	ns	0.6859
Omicron (BNT162b2 dose 2) vs. (ChAdOX1 dose 2)	-173.8	-5103 to 4756	No	ns	0.9997
Test details	**Mean 1**	**Mean 2**	**Mean Diff.**	**SE of diff.**	**n1**
Wuhan (BNT162b2 dose 2) vs. (ChAdOX1 dose 2)	6164	8242	-2079	1877	20
Omicron (BNT162b2 dose 2) vs. (ChAdOX1 dose 2)	91.73	265.5	-173.8	1877	20

medRxiv preprint doi: https://doi.org/10.1101/2022.01.03.21268111; this version posted January 3, 2022. The copyright holder for this preprint (which was not certified by peer review) is the author/funder, who has granted medRxiv a license to display the preprint in perpetuity.
It is made available under a CC-BY-NC-ND 4.0 International license .

Supplementary Table S9: Table of demographics, SARS-CoV-2 positivity status and vaccination status for the population of 34,641 people aged 18 and over, registered as living in NHS Greater Glasgow and Clyde and tested by PCR test for SARS-CoV-2 infection between 6th and 12th December 2021, split by SARS-CoV-2 variant status.

	Negative	*Delta*	*Omicron*
Demographics			
Age on 31st October 2021			
Minimum	18.77	18.85	18.85
1st Quartile	32.83	31.83	29.67
Median	45.06	40.74	37.49
Mean	47.27	41.56	40.17
3rd Quartile	59.13	49.89	49.39
Maximum	103.16	90.51	89.92
Sex			
Female	20091 (91.37%)	1368 (6.22%)	529 (2.41%)
Male	11016 (87.06%)	1165 (9.21%)	472 (3.73%)
SIMD (2016) quartile			
1	12981 (90.78%)	998 (6.98%)	320 (2.24%)
2	5951 (89.48%)	493 (7.41%)	207 (3.11%)
3	4917 (89.92%)	365 (6.68%)	186 (3.40%)
4	6653 (88.36%)	609 (8.09%)	267 (3.55%)
Unknown	605 (87.18%)	68 (9.80%)	21 (3.03%)
SARS-CoV-2 positivity status			
Date of 1st positive PCR test			
Minimum	12/03/2020	21/05/2020	19/04/2020
1st Quartile	04/11/2020	07/12/2021	07/12/2021
Median	18/01/2021	09/12/2021	09/12/2021
Mean	22/02/2021	04/12/2021	18/11/2021
3rd Quartile	20/07/2021	10/12/2021	11/12/2021
Maximum	21/12/2021	12/12/2021	12/12/2021
Previous confirmed SARS-CoV-2 infection status			
No previous infection	26974 (88.71%)	2496 (8.21%)	936 (3.08%)
Had previous infection	4133 (97.59%)	37 (0.87%)	65 (1.53%)
Vaccination status			
Most recent dose			
0	2014 (80.11%)	417 (16.59%)	83 (3.30%)
1	820 (87.61%)	94 (10.04%)	22 (2.35%)
2	15172 (85.38%)	1836 (10.33%)	761 (4.28%)
3	13101 (97.61%)	186 (1.39%)	135 (1.01%)
Most recent vaccine product name			
None	2014 (80.11%)	417 (16.59%)	83 (3.30%)
ChAdOx1	5301 (80.89%)	955 (14.57%)	297 (4.53%)
BNT162b2	18650 (92.95%)	930 (4.63%)	485 (2.42%)
mRNA-1273	5142 (93.34%)	231 (4.19%)	136 (2.47%)
Most recent vaccine dose by variant group and product name			

medRxiv preprint doi: https://doi.org/10.1101/2022.01.03.21268111; this version posted January 3, 2022. The copyright holder for this preprint **(which was not certified by peer review)** is the author/funder, who has granted medRxiv a license to display the preprint in perpetuity.
It is made available under a CC-BY-NC-ND 4.0 International license .

None	*0*	2014 (80.11%)	417 (16.59%)	83 (3.30%)
ChAdOx1	*1*	230 (88.12%)	26 (9.96%)	5 (1.92%)
	2	5071 (80.59%)	929 (14.76%)	292 (4.64%)
BNT162b2	*1*	389 (87.02%)	49 (10.96%)	9 (2.01%)
	2	8113 (87.89%)	746 (8.08%)	372 (4.03%)
	3	10148 (97.70%)	135 (1.30%)	104 (1.00%)
mRNA-1273	*1*	201 (88.16%)	19 (8.33%)	8 (3.51%)
	2	1988 (88.51%)	161 (7.17%)	97 (4.32%)
	3	2953 (97.30%)	51 (1.68%)	31 (1.02%)
Date of most recent dose				
Minimum		10/12/2020	16/01/2021	25/01/2021
1st Quartile		03/07/2021	11/06/2021	18/06/2021
Median		06/09/2021	08/07/2021	23/07/2021
Mean		20/08/2021	11/07/2021	23/07/2021
3rd Quartile		18/10/2021	07/08/2021	24/08/2021
Maximum		21/11/2021	21/11/2021	21/11/2021

Date of most recent dose by variant and dose number									
	Negative			*Delta*			*Omicron*		
	1	*2*	*3*	*1*	*2*	*3*	*1*	*2*	*3*
Minimum	10/12/2020	08/01/2021	20/09/2021	23/01/2021	16/01/2021	24/09/2021	04/02/2021	25/01/2021	23/09/2021
1st Quartile	17/04/2021	29/05/2021	05/10/2021	21/05/2021	07/06/2021	02/10/2021	07/06/2021	14/06/2021	04/10/2021
Median	23/06/2021	11/07/2021	20/10/2021	01/07/2021	03/07/2021	18/10/2021	31/07/2021	12/07/2021	19/10/2021
Mean	25/06/2021	01/07/2021	20/10/2021	30/06/2021	01/07/2021	20/10/2021	20/07/2021	07/07/2021	21/10/2021
3rd Quartile	04/09/2021	10/08/2021	03/11/2021	26/08/2021	29/07/2021	06/11/2021	05/09/2021	06/08/2021	07/11/2021
Maximum	21/11/2021	21/11/2021	21/11/2021	17/11/2021	19/11/2021	21/11/2021	16/11/2021	14/11/2021	21/11/2021

medRxiv preprint doi: https://doi.org/10.1101/2022.01.03.21268111; this version posted January 3, 2022. The copyright holder for this preprint (which was not certified by peer review) is the author/funder, who has granted medRxiv a license to display the preprint in perpetuity.
It is made available under a CC-BY-NC-ND 4.0 International license .

Supplementary Figure S1. HCoV reactivity following two doses of SARS-CoV-2 vaccine. Antibody responses were studied in three groups of individuals (n=24 per group) vaccinated with either BNT162b2, ChAdOx1 or mRNA-1273 by MSD-ECL assay. Responses were measured against full-length spike glycoprotein (Spike) from HCoVs 229E, OC43, NL63 and HKU1 and are expressed as MSD arbitrary units (AU/ml). The response to OC43 was significantly higher in BNT162b2 vaccinates than in ChAdOx1 vaccinates.

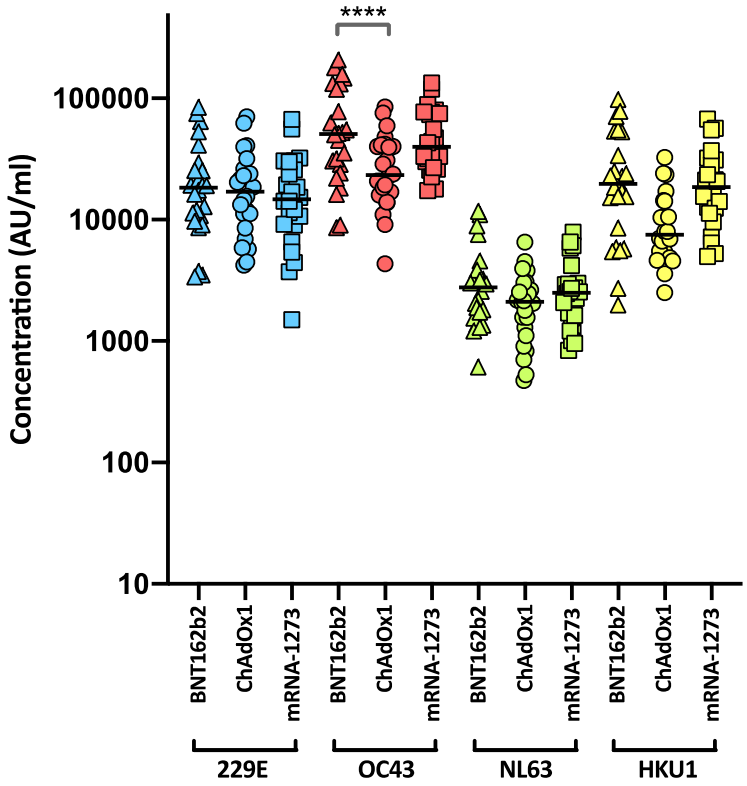

medRxiv preprint doi: https://doi.org/10.1101/2022.01.03.21268111; this version posted January 3, 2022. The copyright holder for this preprint (which was not certified by peer review) is the author/funder, who has granted medRxiv a license to display the preprint in perpetuity.
It is made available under a CC-BY-NC-ND 4.0 International license .

Supplementary Figure S2. Influenza reactivity following two doses of SARS-CoV-2 vaccine. Antibody responses were studied in three groups of individuals (n=24 per group) vaccinated with either BNT162b2, ChAdOx1 or mRNA-1273 by MSD-ECL assay. Responses were measured against haemagglutinins from influenza viruses; influenza A Michigan H1, Hong Kong H3 and Shanghai H7, and influenza B Phuket HA and Brisbane and are expressed as MSD arbitrary units (AU/ml). No significant differences were detected between the vaccine groups for each of the antigens.

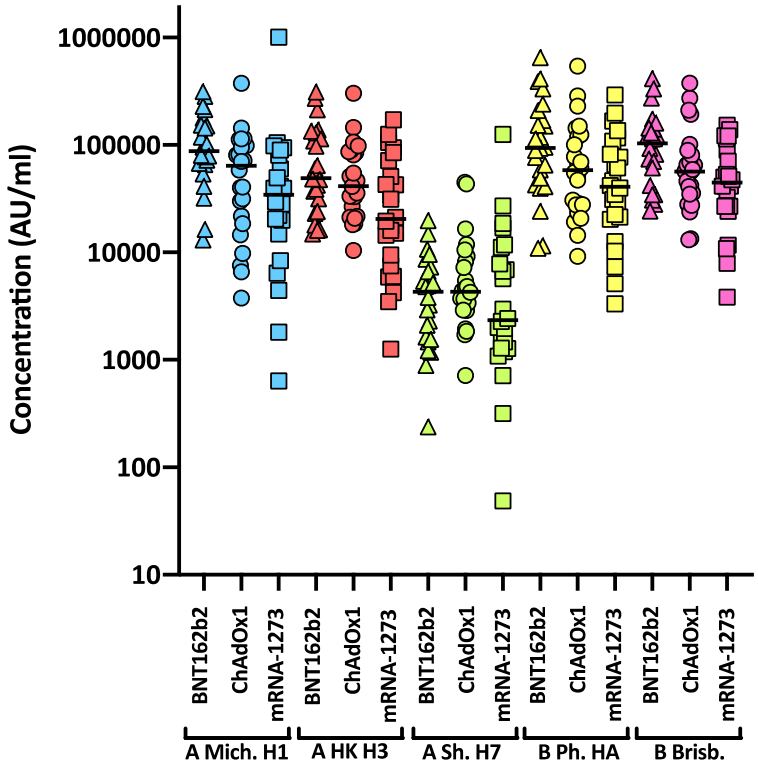

medRxiv preprint doi: https://doi.org/10.1101/2022.01.03.21268111; this version posted January 3, 2022. The copyright holder for this preprint (which was not certified by peer review) is the author/funder, who has granted medRxiv a license to display the preprint in perpetuity.
It is made available under a CC-BY-NC-ND 4.0 International license .

Supplementary Figure S3. HCoV reactivity following third dose of SARS-CoV-2 vaccine. Antibody responses were studied in four groups of individuals primed with two doses of either ChAdOx1 or BNT162b2, followed by a booster of BNT162b2 or mRNA-1273. Responses were measured by MSD-ECL assay against full-length spike glycoprotein (Spike) from HCoVs 229E, OC43, NL63 and HKU1 and are expressed as MSD arbitrary units (AU/ml).

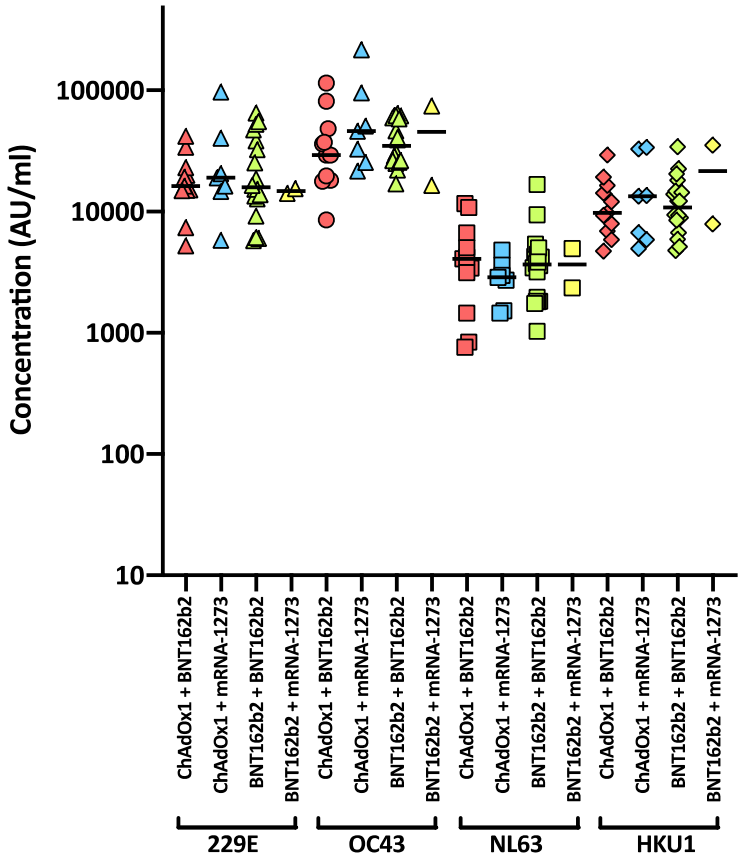

medRxiv preprint doi: https://doi.org/10.1101/2022.01.03.21268111; this version posted January 3, 2022. The copyright holder for this preprint (which was not certified by peer review) is the author/funder, who has granted medRxiv a license to display the preprint in perpetuity.
It is made available under a CC-BY-NC-ND 4.0 International license .

Supplementary Figure S4. Influenza reactivity following third dose of SARS-CoV-2 vaccine. Antibody responses were studied in four groups of individuals primed with two doses of either ChAdOx1 or BNT162b2, followed by a booster of BNT162b2 or mRNA-1273. Responses were measured by MSD-ECL against haemagglutinins from influenza viruses; influenza A Michigan H1, Hong Kong H3 and Shanghai H7, and influenza B Phuket HA and Brisbane and are expressed as MSD arbitrary units (AU/ml). * Significantly different p=0.0413.

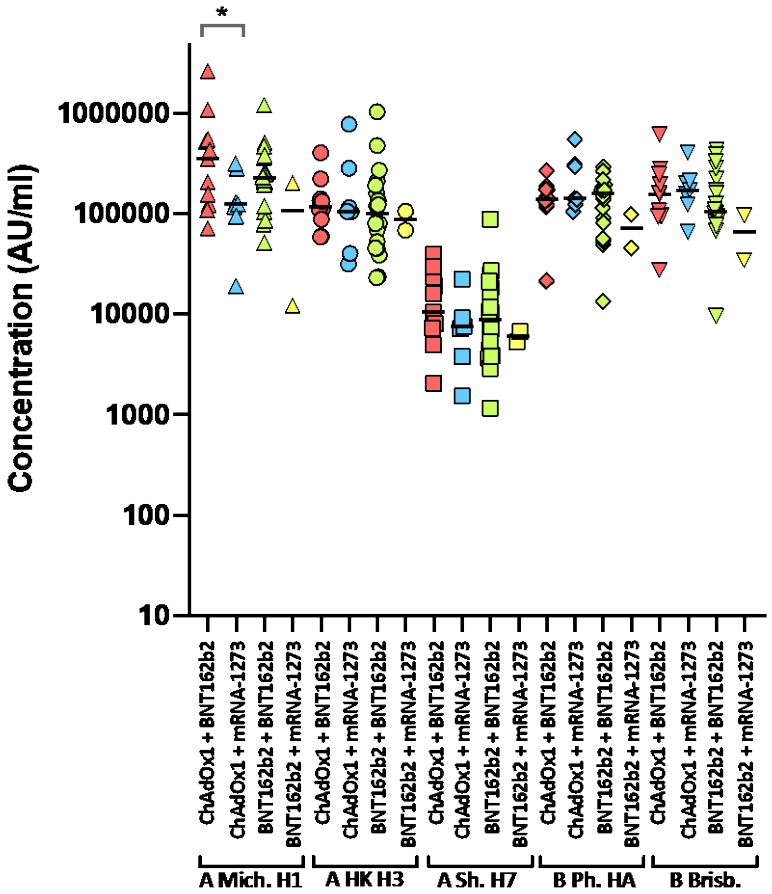

medRxiv preprint doi: https://doi.org/10.1101/2022.01.03.21268111; this version posted January 3, 2022. The copyright holder for this preprint (which was not certified by peer review) is the author/funder, who has granted medRxiv a license to display the preprint in perpetuity.
It is made available under a CC-BY-NC-ND 4.0 International license .

Supplementary Figure S5. Effect of third dose of SARS-CoV-2 vaccine on neutralising antibody titres. Two groups of healthy volunteers vaccinated with two doses of either ChAdOx1 or BNT162b2, were sampled two weeks following a third dose of either BNT162b2 or mRNA-1273. Each point represents the mean of three replicates. Where dose 2 and dose 3 samples were available from the same individual, points are joined by a solid line.

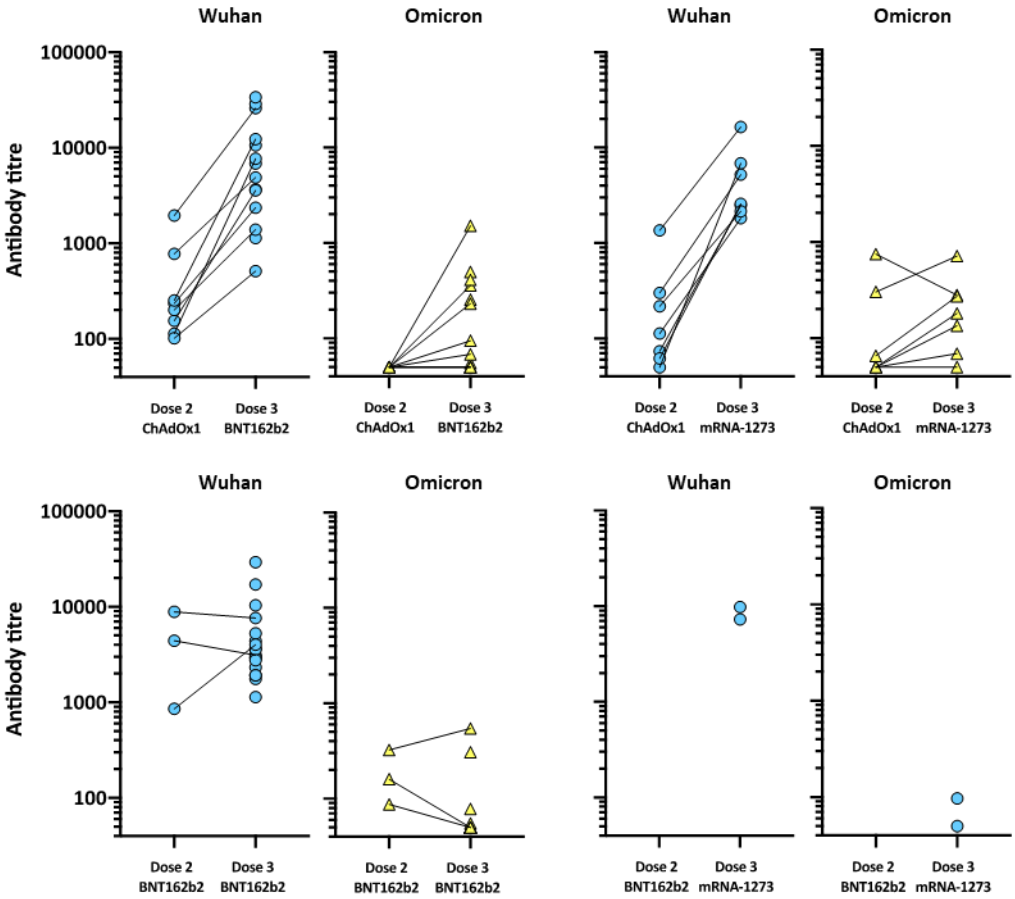

medRxiv preprint doi: https://doi.org/10.1101/2022.01.03.21268111; this version posted January 3, 2022. The copyright holder for this preprint (which was not certified by peer review) is the author/funder, who has granted medRxiv a license to display the preprint in perpetuity.
It is made available under a CC-BY-NC-ND 4.0 International license .

Supplementary Figure S6: Plots of demographics, SARS-CoV-2 positivity status and vaccination status in NHS GG&C. Demographic data for the population of 34,641 people aged 18 and over, registered as living in NHS Greater Glasgow and Clyde and tested by PCR test for SARS-CoV-2 infection between 6th and 12th December 2021, coloured by SARS-CoV-2 variant status. (A) Histogram of age; (B) Barplot of sex; (C) Barplot of SIMD (2016) quartile; (D) Barplot of date of positive SARS-CoV-2 PCR test; (E) Barplot of previous confirmed SARS-CoV-2 infection at least 90 days before most recent positive SARS-CoV-2 PCR test; (F) Barplots of most recent vaccine dose number, split by product name; (G) Barplot of most recent vaccine dose product name; (H) Barplots of time (days) since most recent vaccine dose, split by dose number and product name.

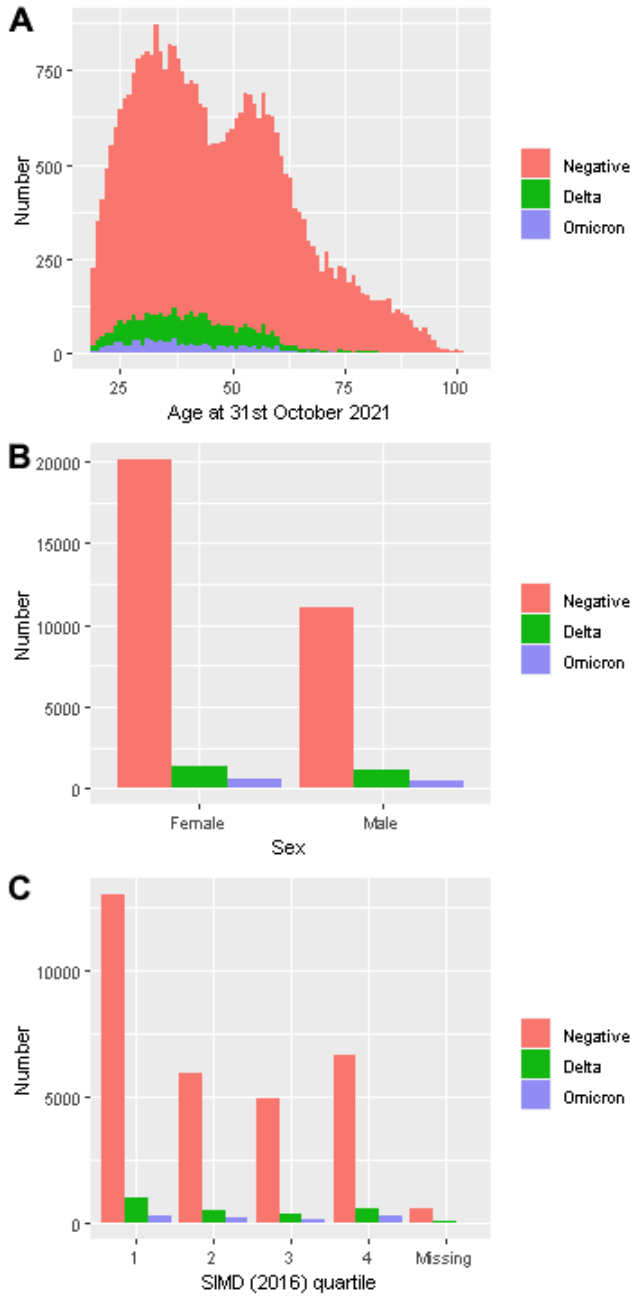

medRxiv preprint doi: https://doi.org/10.1101/2022.01.03.21268111; this version posted January 3, 2022. The copyright holder for this preprint **(which was not certified by peer review)** is the author/funder, who has granted medRxiv a license to display the preprint in perpetuity.
It is made available under a CC-BY-NC-ND 4.0 International license .

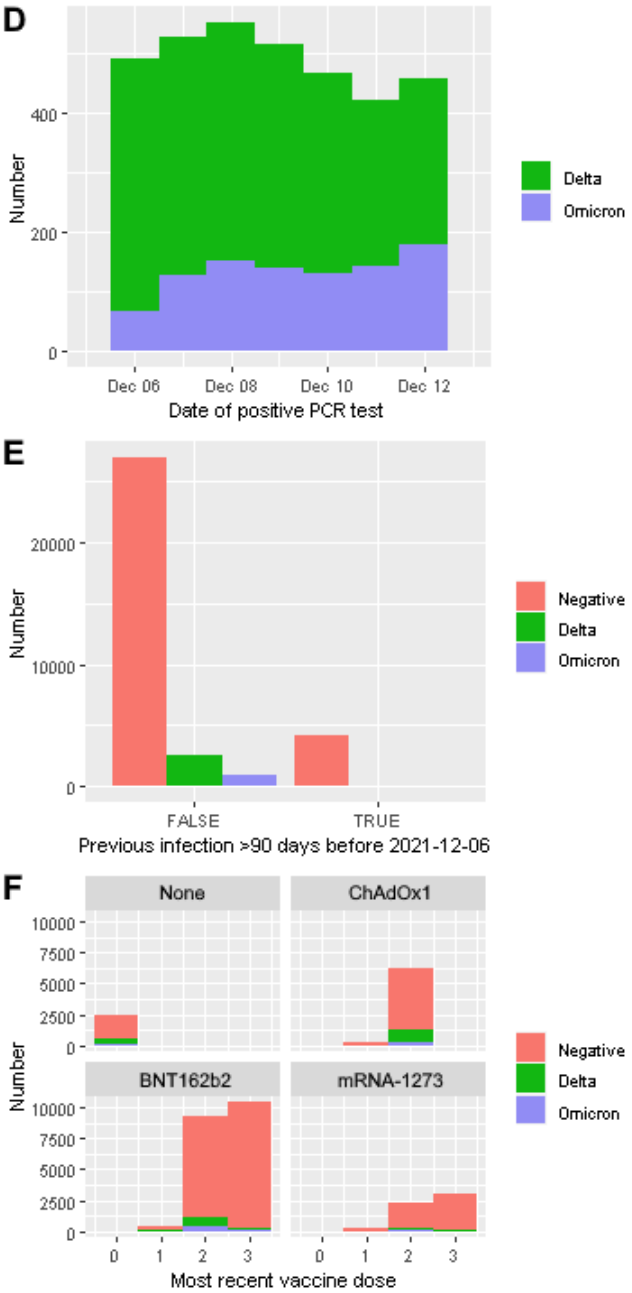

medRxiv preprint doi: https://doi.org/10.1101/2022.01.03.21268111; this version posted January 3, 2022. The copyright holder for this preprint **(which was not certified by peer review)** is the author/funder, who has granted medRxiv a license to display the preprint in perpetuity.
It is made available under a CC-BY-NC-ND 4.0 International license .

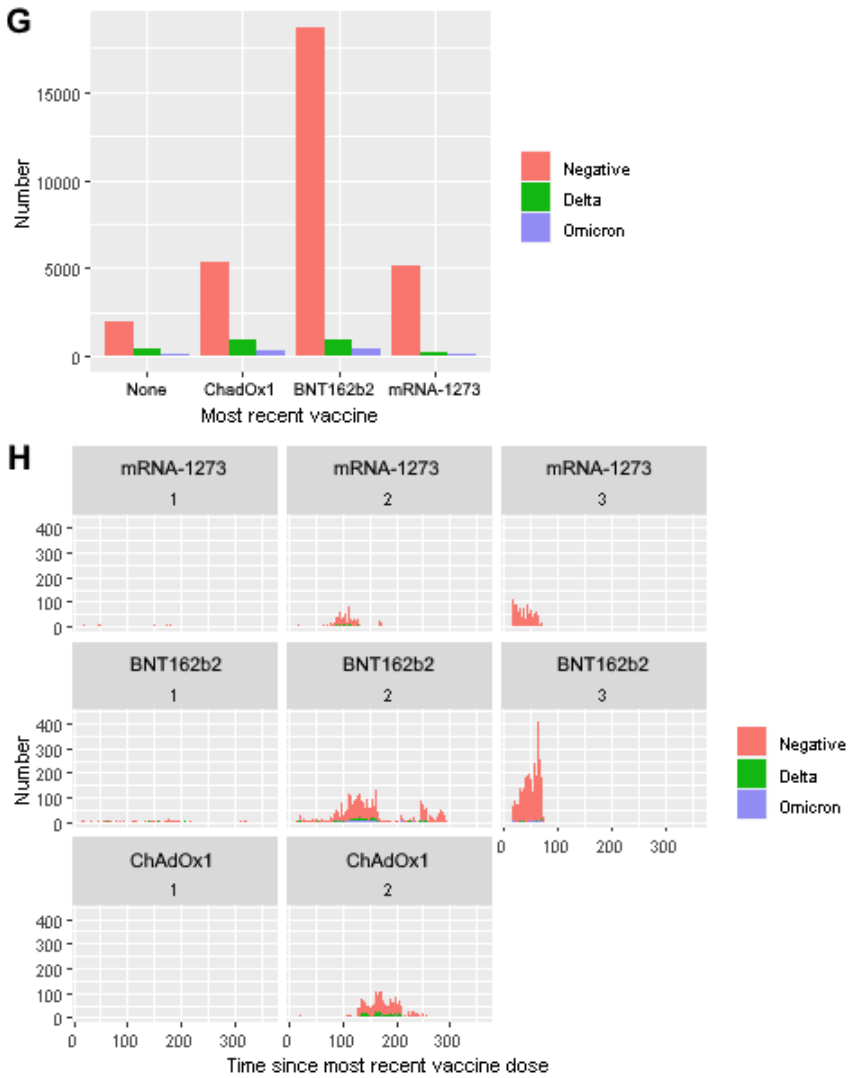

medRxiv preprint doi: https://doi.org/10.1101/2022.01.03.21268111; this version posted January 3, 2022. The copyright holder for this preprint **(which was not certified by peer review)** is the author/funder, who has granted medRxiv a license to display the preprint in perpetuity.
It is made available under a CC-BY-NC-ND 4.0 International license .

Supplementary Figure S7 Isolation of Omicron in cell culture. A. Vero ACE2 TMPRSS2 (VAT) and BHK-hACE2 cells were inoculated with diluted clinical samples. Viral progeny was quantified in the medium 5 dpi by RT-qPCR. B. Aliquots of the medium from samples named 204 and 205 were used to generate a P1 in BHK-hACE2 and Calu-3 cells and, limited to sample 205, a P2 in Calu-3 and Caco2 cells. Viral stocks were quantified by RT-qPCR.

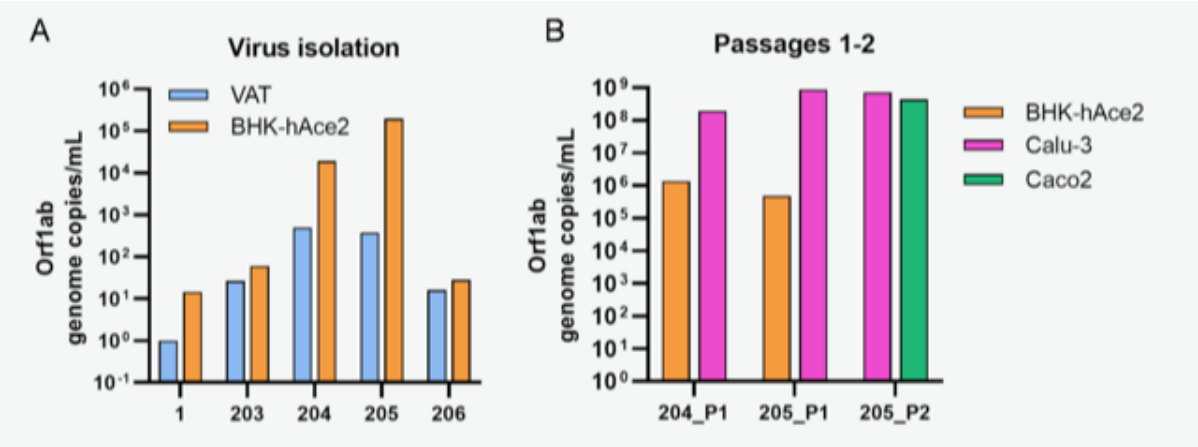

medRxiv preprint doi: https://doi.org/10.1101/2022.01.03.21268111; this version posted January 3, 2022. The copyright holder for this preprint (which was not certified by peer review) is the author/funder, who has granted medRxiv a license to display the preprint in perpetuity.
It is made available under a CC-BY-NC-ND 4.0 International license .

The COVID-19 Genomics UK (COG-UK) consortium

June 2021 V.1

Funding acquisition, Leadership and supervision, Metadata curation, Project administration, Samples and logistics, Sequencing and analysis, Software and analysis tools, and Visualisation:
Dr Samuel C Robson [13, 84]

Funding acquisition, Leadership and supervision, Metadata curation, Project administration, Samples and logistics, Sequencing and analysis, and Software and analysis tools:
Dr Thomas R Connor [11, 74] and Prof Nicholas J Loman [43]

Leadership and supervision, Metadata curation, Project administration, Samples and logistics, Sequencing and analysis, Software and analysis tools, and Visualisation:
Dr Tanya Golubchik [5]

Funding acquisition, Leadership and supervision, Metadata curation, Samples and logistics, Sequencing and analysis, and Visualisation:
Dr Rocio T Martinez Nunez [46]

Funding acquisition, Leadership and supervision, Project administration, Samples and logistics, Sequencing and analysis, and Software and analysis tools:
Dr David Bonsall [5]

Funding acquisition, Leadership and supervision, Project administration, Sequencing and analysis, Software and analysis tools, and Visualisation:
Prof Andrew Rambaut [104]

Funding acquisition, Metadata curation, Project administration, Samples and logistics, Sequencing and analysis, and Software and analysis tools:
Dr Luke B Snell [12]

Leadership and supervision, Metadata curation, Project administration, Samples and logistics, Software and analysis tools, and Visualisation:
Rich Livett [116]

Funding acquisition, Leadership and supervision, Metadata curation, Project administration, and Samples and logistics:
Dr Catherine Ludden [20, 70]

Funding acquisition, Leadership and supervision, Metadata curation, Samples and logistics, and Sequencing and analysis:
Dr Sally Corden [74] and Dr Eleni Nastouli [96, 95, 30]

Funding acquisition, Leadership and supervision, Metadata curation, Sequencing and analysis, and Software and analysis tools:
Dr Gaia Nebbia [12]

Funding acquisition, Leadership and supervision, Project administration, Samples and logistics, and Sequencing and analysis:
Ian Johnston [116]

medRxiv preprint doi: https://doi.org/10.1101/2022.01.03.21268111; this version posted January 3, 2022. The copyright holder for this preprint (which was not certified by peer review) is the author/funder, who has granted medRxiv a license to display the preprint in perpetuity.
It is made available under a CC-BY-NC-ND 4.0 International license .

Leadership and supervision, Metadata curation, Project administration, Samples and logistics, and Sequencing and analysis:
Prof Katrina Lythgoe [5], Dr M. Estee Torok [19,20] and Prof Ian G Goodfellow [24]
Leadership and supervision, Metadata curation, Project administration, Samples and logistics, and Visualisation:
Dr Jacqui A Prieto [97,82] and Dr Kordo Saeed [97,83]

Leadership and supervision, Metadata curation, Project administration, Sequencing and analysis, and Software and analysis tools:
Dr David K Jackson [116]

Leadership and supervision, Metadata curation, Samples and logistics, Sequencing and analysis, and Visualisation:
Dr Catherine Houlihan [96,94]

Leadership and supervision, Metadata curation, Sequencing and analysis, Software and analysis tools, and Visualisation:
Dr Dan Frampton [94,95]

Metadata curation, Project administration, Samples and logistics, Sequencing and analysis, and Software and analysis tools:
Dr William L Hamilton [19] and Dr Adam A Witney [41]

Funding acquisition, Samples and logistics, Sequencing and analysis, and Visualisation:
Dr Giselda Bucca [101]

Funding acquisition, Leadership and supervision, Metadata curation, and Project administration:
Dr Cassie F Pope [40,41]

Funding acquisition, Leadership and supervision, Metadata curation, and Samples and logistics:
Dr Catherine Moore [74]

Funding acquisition, Leadership and supervision, Metadata curation, and Sequencing and analysis:
Prof Emma C Thomson [53]

Funding acquisition, Leadership and supervision, Project administration, and Samples and logistics:
Dr Ewan M Harrison [116,102]

Funding acquisition, Leadership and supervision, Sequencing and analysis, and Visualisation:
Prof Colin P Smith [101]

Leadership and supervision, Metadata curation, Project administration, and Sequencing and analysis:
Fiona Rogan [77]

Leadership and supervision, Metadata curation, Project administration, and Samples and logistics:
Shaun M Beckwith [6], Abigail Murray [6], Dawn Singleton [6], Dr Kirstine Eastick [37], Dr Liz A Sheridan [98], Paul Randell [99], Dr Leigh M Jackson [105], Dr Cristina V Ariani [116] and Dr Sónia Gonçalves [116]

medRxiv preprint doi: https://doi.org/10.1101/2022.01.03.21268111; this version posted January 3, 2022. The copyright holder for this preprint (which was not certified by peer review) is the author/funder, who has granted medRxiv a license to display the preprint in perpetuity.
It is made available under a CC-BY-NC-ND 4.0 International license .

Leadership and supervision, Metadata curation, Samples and logistics, and Sequencing and analysis:
Dr Derek J Fairley [3, 77], Prof Matthew W Loose [18] and Joanne Watkins [74]

Leadership and supervision, Metadata curation, Samples and logistics, and Visualisation:
Dr Samuel Moses [25, 106]

Leadership and supervision, Metadata curation, Sequencing and analysis, and Software and analysis tools:
Dr Sam Nicholls [43], Dr Matthew Bull [74] and Dr Roberto Amato [116]

Leadership and supervision, Project administration, Samples and logistics, and Sequencing and analysis:
Prof Darren L Smith [36, 65, 66]

Leadership and supervision, Sequencing and analysis, Software and analysis tools, and Visualisation:
Prof David M Aanensen [14, 116] and Dr Jeffrey C Barrett [116]

Metadata curation, Project administration, Samples and logistics, and Sequencing and analysis:
Dr Dinesh Aggarwal [20, 116, 70], Dr James G Shepherd [53], Dr Martin D Curran [71] and Dr Surendra Parmar [71]

Metadata curation, Project administration, Sequencing and analysis, and Software and analysis tools:
Dr Matthew D Parker [109]

Metadata curation, Samples and logistics, Sequencing and analysis, and Software and analysis tools:
Dr Catryn Williams [74]

Metadata curation, Samples and logistics, Sequencing and analysis, and Visualisation:
Dr Sharon Glaysher [68]

Metadata curation, Sequencing and analysis, Software and analysis tools, and Visualisation:
Dr Anthony P Underwood [14, 116], Dr Matthew Bashton [36, 65], Dr Nicole Pacchiarini [74], Dr Katie F Loveson [84] and Matthew Byott [95, 96]

Project administration, Sequencing and analysis, Software and analysis tools, and Visualisation:
Dr Alessandro M Carabelli [20]

Funding acquisition, Leadership and supervision, and Metadata curation:
Dr Kate E Templeton [56, 104]

Funding acquisition, Leadership and supervision, and Project administration:
Dr Thushan I de Silva [109], Dr Dennis Wang [109], Dr Cordelia F Langford [116] and John Sillitoe [116]

Funding acquisition, Leadership and supervision, and Samples and logistics:
Prof Rory N Gunson [55]

Funding acquisition, Leadership and supervision, and Sequencing and analysis:

medRxiv preprint doi: https://doi.org/10.1101/2022.01.03.21268111; this version posted January 3, 2022. The copyright holder for this preprint (which was not certified by peer review) is the author/funder, who has granted medRxiv a license to display the preprint in perpetuity.
It is made available under a CC-BY-NC-ND 4.0 International license .

Dr Simon Cottrell [74], Dr Justin O'Grady [75, 103] and Prof Dominic Kwiatkowski [116, 108]

Leadership and supervision, Metadata curation, and Project administration:
Dr Patrick J Lillie [37]

Leadership and supervision, Metadata curation, and Samples and logistics:
Dr Nicholas Cortes [33], Dr Nathan Moore [33], Dr Claire Thomas [33], Phillipa J Burns [37], Dr Tabitha W Mahungu [80] and Steven Liggett [86]

Leadership and supervision, Metadata curation, and Sequencing and analysis:
Angela H Beckett [13, 81] and Prof Matthew TG Holden [73]

Leadership and supervision, Project administration, and Samples and logistics:
Dr Lisa J Levett [34], Dr Husam Osman [70, 35] and Dr Mohammed O Hassan-Ibrahim [99]

Leadership and supervision, Project administration, and Sequencing and analysis:
Dr David A Simpson [77]

Leadership and supervision, Samples and logistics, and Sequencing and analysis:
Dr Meera Chand [72], Prof Ravi K Gupta [102], Prof Alistair C Darby [107] and Prof Steve Paterson [107]

Leadership and supervision, Sequencing and analysis, and Software and analysis tools:
Prof Oliver G Pybus [23], Dr Erik M Volz [39], Prof Daniela de Angelis [52], Prof David L Robertson [53], Dr Andrew J Page [75] and Dr Inigo Martincorena [116]

Leadership and supervision, Sequencing and analysis, and Visualisation:
Dr Louise Aigrain [116] and Dr Andrew R Bassett [116]

Metadata curation, Project administration, and Samples and logistics:
Dr Nick Wong [50], Dr Yusri Taha [89], Michelle J Erkiert [99] and Dr Michael H Spencer Chapman [116, 102]

Metadata curation, Project administration, and Sequencing and analysis:
Dr Rebecca Dewar [56] and Martin P McHugh [56, 111]

Metadata curation, Project administration, and Software and analysis tools:
Siddharth Mookerjee [38, 57]

Metadata curation, Project administration, and Visualisation:
Stephen Aplin [97], Matthew Harvey [97], Thea Sass [97], Dr Helen Umpleby [97] and Helen Wheeler [97]

Metadata curation, Samples and logistics, and Sequencing and analysis:
Dr James P McKenna [3], Dr Ben Warne [9], Joshua F Taylor [22], Yasmin Chaudhry [24], Rhys Izuagbe [24], Dr Aminu S Jahun [24], Dr Gregory R Young [36, 65], Dr Claire McMurray [43], Dr Clare M McCann [65, 66], Dr Andrew Nelson [65, 66] and Scott Elliott [68]

Metadata curation, Samples and logistics, and Visualisation:
Hannah Lowe [25]

Metadata curation, Sequencing and analysis, and Software and analysis tools:
Dr Anna Price [11], Matthew R Crown [65], Dr Sara Rey [74], Dr Sunando Roy [96] and Dr Ben Temperton [105]

medRxiv preprint doi: https://doi.org/10.1101/2022.01.03.21268111; this version posted January 3, 2022. The copyright holder for this preprint (which was not certified by peer review) is the author/funder, who has granted medRxiv a license to display the preprint in perpetuity.
It is made available under a CC-BY-NC-ND 4.0 International license .

Metadata curation, Sequencing and analysis, and Visualisation:
Dr Sharif Shaaban [73] and Dr Andrew R Hesketh [101]

Project administration, Samples and logistics, and Sequencing and analysis:
Dr Kenneth G Laing [41], Dr Irene M Monahan [41] and Dr Judith Heaney [95, 96, 34]

Project administration, Samples and logistics, and Visualisation:
Dr Emanuela Pelosi [97], Siona Silviera [97] and Dr Eleri Wilson-Davies [97]

Samples and logistics, Software and analysis tools, and Visualisation:
Dr Helen Fryer [5]

Sequencing and analysis, Software and analysis tools, and Visualization:
Dr Helen Adams [4], Dr Louis du Plessis [23], Dr Rob Johnson [39], Dr William T Harvey [53, 42], Dr Joseph Hughes [53], Dr Richard J Orton [53], Dr Lewis G Spurgin [59], Dr Yann Bourgeois [81], Dr Chris Ruis [102], Áine O'Toole [104], Marina Gourtovaia [116] and Dr Theo Sanderson [116]

Funding acquisition, and Leadership and supervision:
Dr Christophe Fraser [5], Dr Jonathan Edgeworth [12], Prof Judith Breuer [96, 29], Dr Stephen L Michell [105] and Prof John A Todd [115]

Funding acquisition, and Project administration:
Michaela John [10] and Dr David Buck [115]

Leadership and supervision, and Metadata curation:
Dr Kavitha Gajee [37] and Dr Gemma L Kay [75]

Leadership and supervision, and Project administration:
Prof Sharon J Peacock [20, 70] and David Heyburn [74]

Leadership and supervision, and Samples and logistics:
Katie Kitchman [37], Prof Alan McNally [43, 93], David T Pritchard [50], Dr Samir Dervisevic [58], Dr Peter Muir [70], Dr Esther Robinson [70, 35], Dr Barry B Vipond [70], Newara A Ramadan [78], Dr Christopher Jeanes [90], Danni Weldon [116], Jana Catalan [118] and Neil Jones [118]

Leadership and supervision, and Sequencing and analysis:
Dr Ana da Silva Filipe [53], Dr Chris Williams [74], Marc Fuchs [77], Dr Julia Miskelly [77], Dr Aaron R Jeffries [105], Karen Oliver [116] and Dr Naomi R Park [116]

Metadata curation, and Samples and logistics:
Amy Ash [1], Cherian Koshy [1], Magdalena Barrow [7], Dr Sarah L Buchan [7], Dr Anna Mantzouratou [7], Dr Gemma Clark [15], Dr Christopher W Holmes [16], Sharon Campbell [17], Thomas Davis [21], Ngee Keong Tan [22], Dr Julianne R Brown [29], Dr Kathryn A Harris [29, 2], Stephen P Kidd [33], Dr Paul R Grant [34], Dr Li Xu-McCrae [35], Dr Alison Cox [38, 63], Pinglawathee Madona [38, 63], Dr Marcus Pond [38, 63], Dr Paul A Randell [38, 63], Karen T Withell [48], Cheryl Williams [51], Dr Clive Graham [60], Rebecca Denton-Smith [62], Emma Swindells [62], Robyn Turnbull [62], Dr Tim J Sloan [67], Dr Andrew Bosworth [70, 35], Stephanie Hutchings [70], Hannah M Pymont [70], Dr Anna Casey [76], Dr Liz Ratcliffe [76], Dr Christopher R Jones [79, 105], Dr Bridget A Knight [79, 105], Dr Tanzina Haque [80], Dr Jennifer Hart [80], Dr Dianne Irish-Tavares [80], Eric Witele [80], Craig Mower [86], Louisa K Watson [86], Jennifer Collins [89], Gary Eltringham [89], Dorian Crudgington [98], Ben Macklin [98], Prof Miren Iturriza-Gomara [107], Dr Anita O Lucaci [107] and Dr Patrick C McClure [113]

medRxiv preprint doi: https://doi.org/10.1101/2022.01.03.21268111; this version posted January 3, 2022. The copyright holder for this preprint (which was not certified by peer review) is the author/funder, who has granted medRxiv a license to display the preprint in perpetuity.
It is made available under a CC-BY-NC-ND 4.0 International license .

Metadata curation, and Sequencing and analysis:
Matthew Carlile [18], Dr Nadine Holmes [18], Dr Christopher Moore [18], Dr Nathaniel Storey [29], Dr Stefan Rooke [73], Dr Gonzalo Yebra [73], Dr Noel Craine [74], Malorie Perry [74], Dr Nabil-Fareed Alikhan [75], Dr Stephen Bridgett [77], Kate F Cook [84], Christopher Fearn [84], Dr Salman Goudarzi [84], Prof Ronan A Lyons [88], Dr Thomas Williams [104], Dr Sam T Haldenby [107], Jillian Durham [116] and Dr Steven Leonard [116]

Metadata curation, and Software and analysis tools:
Robert M Davies [116]

Project administration, and Samples and logistics:
Dr Rahul Batra [12], Beth Blane [20], Dr Moira J Spyer [30, 95, 96], Perminder Smith [32, 112], Mehmet Yavus [85, 109], Dr Rachel J Williams [96], Dr Adhyana IK Mahanama [97], Dr Buddhini Samaraweera [97], Sophia T Girgis [102], Samantha E Hansford [109], Dr Angie Green [115], Dr Charlotte Beaver [116], Katherine L Bellis [116, 102], Matthew J Dorman [116], Sally Kay [116], Liam Prestwood [116] and Dr Shavanthi Rajatileka [116]

Project administration, and Sequencing and analysis:
Dr Joshua Quick [43]

Project administration, and Software and analysis tools:
Radoslaw Poplawski [43]

Samples and logistics, and Sequencing and analysis:
Dr Nicola Reynolds [8], Andrew Mack [11], Dr Arthur Morriss [11], Thomas Whalley [11], Bindi Patel [12], Dr Iliana Georgana [24], Dr Myra Hosmillo [24], Malte L Pinckert [24], Dr Joanne Stockton [43], Dr John H Henderson [65], Amy Hollis [65], Dr William Stanley [65], Dr Wen C Yew [65], Dr Richard Myers [72], Dr Alicia Thornton [72], Alexander Adams [74], Tara Annett [74], Dr Hibo Asad [74], Alec Birchley [74], Jason Coombes [74], Johnathan M Evans [74], Laia Fina [74], Bree Gatica-Wilcox [74], Lauren Gilbert [74], Lee Graham [74], Jessica Hey [74], Ember Hilvers [74], Sophie Jones [74], Hannah Jones [74], Sara Kumziene-Summerhayes [74], Dr Caoimhe McKerr [74], Jessica Powell [74], Georgia Pugh [74], Sarah Taylor [74], Alexander J Trotter [75], Charlotte A Williams [96], Leanne M Kermack [102], Benjamin H Foulkes [109], Marta Gallis [109], Hailey R Hornsby [109], Stavroula F Louka [109], Dr Manoj Pohare [109], Paige Wolverson [109], Peijun Zhang [109], George MacIntyre-Cockett [115], Amy Trebes [115], Dr Robin J Moll [116], Lynne Ferguson [117], Dr Emily J Goldstein [117], Dr Alasdair Maclean [117] and Dr Rachael Tomb [117]

Samples and logistics, and Software and analysis tools:
Dr Igor Starinskij [53]

Sequencing and analysis, and Software and analysis tools:
Laura Thomson [5], Joel Southgate [11, 74], Dr Moritz UG Kraemer [23], Dr Jayna Raghwani [23], Dr Alex E Zarebski [23], Olivia Boyd [39], Lily Geidelberg [39], Dr Chris J Illingworth [52], Dr Chris Jackson [52], Dr David Pascall [52], Dr Sreenu Vattipally [53], Timothy M Freeman [109], Dr Sharon N Hsu [109], Dr Benjamin B Lindsey [109], Dr Keith James [116], Kevin Lewis [116], Gerry Tonkin-Hill [116] and Dr Jaime M Tovar-Corona [116]

Sequencing and analysis, and Visualisation:
MacGregor Cox [20]

Software and analysis tools, and Visualisation:
Dr Khalil Abudahab [14, 116], Mirko Menegazzo [14], Ben EW Taylor MEng [14, 116], Dr Corin A Yeats [14], Afrida Mukaddas [53], Derek W Wright [53], Dr Leonardo de Oliveira Martins [75], Dr Rachel Colquhoun [104], Verity

medRxiv preprint doi: https://doi.org/10.1101/2022.01.03.21268111; this version posted January 3, 2022. The copyright holder for this preprint (which was not certified by peer review) is the author/funder, who has granted medRxiv a license to display the preprint in perpetuity.
It is made available under a CC-BY-NC-ND 4.0 International license .

Hill [104], Dr Ben Jackson [104], Dr JT McCrone [104], Dr Nathan Medd [104], Dr Emily Scher [104] and Jon-Paul Keatley [116]

Leadership and supervision:

Dr Tanya Curran [3], Dr Sian Morgan [10], Prof Patrick Maxwell [20], Prof Ken Smith [20], Dr Sahar Eldirdiri [21], Anita Kenyon [21], Prof Alison H Holmes [38,57], Dr James R Price [38,57], Dr Tim Wyatt [69], Dr Alison E Mather [75], Dr Timofey Skvortsov [77] and Prof John A Hartley [96]

Metadata curation:

Prof Martyn Guest [11], Dr Christine Kitchen [11], Dr Ian Merrick [11], Robert Munn [11], Dr Beatrice Bertolusso [33], Dr Jessica Lynch [33], Dr Gabrielle Vernet [33], Stuart Kirk [34], Dr Elizabeth Wastnedge [56], Dr Rachael Stanley [58], Giles Idle [64], Dr Declan T Bradley [69,77], Dr Jennifer Poyner [79] and Matilde Mori [110]

Project administration:

Owen Jones [11], Victoria Wright [18], Ellena Brooks [20], Carol M Churcher [20], Mireille Fragakis [20], Dr Katerina Galai [20,70], Dr Andrew Jermy [20], Sarah Judges [20], Georgina M McManus [20], Kim S Smith [20], Dr Elaine Westwick [20], Dr Stephen W Attwood [23], Dr Frances Bolt [38,57], Dr Alisha Davies [74], Elen De Lacy [74], Fatima Downing [74], Sue Edwards [74], Lizzie Meadows [75], Sarah Jeremiah [97], Dr Nikki Smith [109] and Luke Foulser [116]

Samples and logistics:

Dr Themoula Charalampous [12,46], Amita Patel [12], Dr Louise Berry [15], Dr Tim Boswell [15], Dr Vicki M Fleming [15], Dr Hannah C Howson-Wells [15], Dr Amelia Joseph [15], Manjinder Khakh [15], Dr Michelle M Lister [15], Paul W Bird [16], Karlie Fallon [16], Thomas Helmer [16], Dr Claire L McMurray [16], Mina Odedra [16], Jessica Shaw [16], Dr Julian W Tang [16], Nicholas J Willford [16], Victoria Blakey [17], Dr Veena Raviprakash [17], Nicola Sheriff [17], Lesley-Anne Williams [17], Theresa Feltwell [20], Dr Luke Bedford [26], Dr James S Cargill [27], Warwick Hughes [27], Dr Jonathan Moore [28], Susanne Stonehouse [28], Laura Atkinson [29], Jack CD Lee [29], Dr Divya Shah [29], Adela Alcolea-Medina [32,112], Natasha Ohemeng-Kumi [32,112], John Ramble [32,112], Jasveen Sehmi [32,112], Dr Rebecca Williams [33], Wendy Chatterton [34], Monika Pusok [34], William Everson [37], Anibolina Castigador [44], Emily Macnaughton [44], Dr Kate El Bouzidi [45], Dr Temi Lampejo [45], Dr Malur Sudhanva [45], Cassie Breen [47], Dr Graciela Sluga [48], Dr Shazaad SY Ahmad [49,70], Dr Ryan P George [49], Dr Nicholas W Machin [49,70], Debbie Binns [50], Victoria James [50], Dr Rachel Blacow [55], Dr Lindsay Coupland [58], Dr Louise Smith [59], Dr Edward Barton [60], Debra Padgett [60], Garren Scott [60], Dr Aidan Cross [61], Dr Mariyam Mirfenderesky [61], Jane Greenaway [62], Kevin Cole [64], Phillip Clarke [67], Nichola Duckworth [67], Sarah Walsh [67], Kelly Bicknell [68], Robert Impey [68], Dr Sarah Wyllie [68], Richard Hopes [70], Dr Chloe Bishop [72], Dr Vicki Chalker [72], Dr Ian Harrison [72], Laura Gifford [74], Dr Zoltan Molnar [77], Dr Cressida Auckland [79], Dr Cariad Evans [85,109], Dr Kate Johnson [85,109], Dr David G Partridge [85,109], Dr Mohammad Raza [85,109], Paul Baker [86], Prof Stephen Bonner [86], Sarah Essex [86], Leanne J Murray [86], Andrew I Lawton [87], Dr Shirelle Burton-Fanning [89], Dr Brendan AI Payne [89], Dr Sheila Waugh [89], Andrea N Gomes [91], Maimuna Kimuli [91], Darren R Murray [91], Paula Ashfield [92], Dr Donald Dobie [92], Dr Fiona Ashford [93], Dr Angus Best [93], Dr Liam Crawford [93], Dr Nicola Cumley [93], Dr Megan Mayhew [93], Dr Oliver Megram [93], Dr Jeremy Mirza [93], Dr Emma Moles-Garcia [93], Dr Benita Percival [93], Megan Driscoll [96], Leah Ensell [96], Dr Helen L Lowe [96], Laurentiu Maftei [96], Matteo Mondani [96], Nicola J Chaloner [99], Benjamin J Cogger [99], Lisa J Easton [99], Hannah Huckson [99], Jonathan Lewis [99], Sarah Lowdon [99], Cassandra S Malone [99], Florence Munemo [99], Manasa Mutingwende [99], Roberto Nicodemi [99], Olga Podplomyk [99], Thomas Somassa [99], Dr Andrew Beggs [100], Dr Alex Richter [100], Claire Cormie [102], Joana Dias [102], Sally Forrest [102], Dr Ellen E Higginson [102], Mailis Maes [102], Jamie Young [102], Dr Rose K Davidson [103], Kathryn A Jackson [107], Dr Lance Turtle [107], Dr Alexander J Keeley [109], Prof Jonathan Ball [113], Timothy Byaruhanga [113], Dr

medRxiv preprint doi: https://doi.org/10.1101/2022.01.03.21268111; this version posted January 3, 2022. The copyright holder for this preprint (which was not certified by peer review) is the author/funder, who has granted medRxiv a license to display the preprint in perpetuity.
It is made available under a CC-BY-NC-ND 4.0 International license .

Joseph G Chappell [113], Jayasree Dey [113], Jack D Hill [113], Emily J Park [113], Arezou Fanaie [114], Rachel A Hilson [114], Geraldine Yaze [114] and Stephanie Lo [116]

Sequencing and analysis:
Safiah Afifi [10], Robert Beer [10], Joshua Maksimovic [10], Kathryn McCluggage [10], Karla Spellman [10], Catherine Bresner [11], William Fuller [11], Dr Angela Marchbank [11], Trudy Workman [11], Dr Ekaterina Shelest [13,81], Dr Johnny Debebe [18], Dr Fei Sang [18], Dr Marina Escalera Zamudio [23], Dr Sarah Francois [23], Bernardo Gutierrez [23], Dr Tetyana I Vasylyeva [23], Dr Flavia Flaviani [31], Dr Manon Ragonnet-Cronin [39], Dr Katherine L Smollett [42], Alice Broos [53], Daniel Mair [53], Jenna Nichols [53], Dr Kyriaki Nomikou [53], Dr Lily Tong [53], Ioulia Tsatsani [53], Prof Sarah O'Brien [54], Prof Steven Rushton [54], Dr Roy Sanderson [54], Dr Jon Perkins [55], Seb Cotton [56], Abbie Gallagher [56], Dr Elias Allara [70,102], Clare Pearson [70,102], Dr David Bibby [72], Dr Gavin Dabrera [72], Dr Nicholas Ellaby [72], Dr Eileen Gallagher [72], Dr Jonathan Hubb [72], Dr Angie Lackenby [72], Dr David Lee [72], Nikos Manesis [72], Dr Tamyo Mbisa [72], Dr Steven Platt [72], Katherine A Twohig [72], Dr Mari Morgan [74], Alp Aydin [75], David J Baker [75], Dr Ebenezer Foster-Nyarko [75], Dr Sophie J Prosolek [75], Steven Rudder [75], Chris Baxter [77], Sílvia F Carvalho [77], Dr Deborah Lavin [77], Dr Arun Mariappan [77], Dr Clara Radulescu [77], Dr Aditi Singh [77], Miao Tang [77], Helen Morcrette [79], Nadua Bayzid [96], Marius Cotic [96], Dr Carlos E Balcazar [104], Dr Michael D Gallagher [104], Dr Daniel Maloney [104], Thomas D Stanton [104], Dr Kathleen A Williamson [104], Dr Robin Manley [105], Michelle L Michelsen [105], Dr Christine M Sambles [105], Dr David J Studholme [105], Joanna Warwick-Dugdale [105], Richard Eccles [107], Matthew Gemmell [107], Dr Richard Gregory [107], Dr Margaret Hughes [107], Charlotte Nelson [107], Dr Lucille Rainbow [107], Dr Edith E Vamos [107], Hermione J Webster [107], Dr Mark Whitehead [107], Claudia Wierzbicki [107], Dr Adrienn Angyal [109], Dr Luke R Green [109], Dr Max Whiteley [109], Emma Betteridge [116], Dr Iraad F Bronner [116], Ben W Farr [116], Scott Goodwin [116], Dr Stefanie V Lensing [116], Shane A McCarthy [116,102], Dr Michael A Quail [116], Diana Rajan [116], Dr Nicholas M Redshaw [116], Carol Scott [116], Lesley Shirley [116] and Scott AJ Thurston [116]

Software and analysis tools:
Dr Will Rowe [43], Amy Gaskin [74], Dr Thanh Le-Viet [75], James Bonfield [116], Jennifier Liddle [116] and Andrew Whitwham [116]

1 Barking, Havering and Redbridge University Hospitals NHS Trust, **2** Barts Health NHS Trust, **3** Belfast Health & Social Care Trust, **4** Betsi Cadwaladr University Health Board, **5** Big Data Institute, Nuffield Department of Medicine, University of Oxford, **6** Blackpool Teaching Hospitals NHS Foundation Trust, **7** Bournemouth University, **8** Cambridge Stem Cell Institute, University of Cambridge, **9** Cambridge University Hospitals NHS Foundation Trust, **10** Cardiff and Vale University Health Board, **11** Cardiff University, **12** Centre for Clinical Infection and Diagnostics Research, Department of Infectious Diseases, Guy's and St Thomas' NHS Foundation Trust, **13** Centre for Enzyme Innovation, University of Portsmouth, **14** Centre for Genomic Pathogen Surveillance, University of Oxford, **15** Clinical Microbiology Department, Queens Medical Centre, Nottingham University Hospitals NHS Trust, **16** Clinical Microbiology, University Hospitals of Leicester NHS Trust, **17** County Durham and Darlington NHS Foundation Trust, **18** Deep Seq, School of Life Sciences, Queens Medical Centre, University of Nottingham, **19** Department of Infectious Diseases and Microbiology, Cambridge University Hospitals NHS Foundation Trust, **20** Department of Medicine, University of Cambridge, **21** Department of Microbiology, Kettering General Hospital, **22** Department of Microbiology, South West London Pathology, **23** Department of Zoology, University of Oxford, **24** Division of Virology, Department of Pathology, University of Cambridge, **25** East Kent Hospitals University NHS Foundation Trust, **26** East Suffolk and North Essex NHS Foundation Trust, **27** East Sussex Healthcare NHS Trust, **28** Gateshead Health NHS Foundation Trust, **29** Great Ormond Street Hospital for Children NHS Foundation Trust, **30** Great Ormond Street Institute of Child Health (GOS ICH), University College London (UCL), **31** Guy's and St. Thomas' Biomedical Research Centre, **32** Guy's and St. Thomas' NHS Foundation Trust, **33** Hampshire Hospitals NHS Foundation Trust, **34** Health Services Laboratories, **35** Heartlands Hospital, Birmingham, **36** Hub for Biotechnology in the Built Environment, Northumbria University, **37** Hull University Teaching Hospitals NHS Trust, **38** Imperial College Healthcare NHS Trust, **39** Imperial College London, **40** Infection Care Group, St George's University Hospitals NHS Foundation Trust, **41** Institute for Infection and Immunity, St George's University of London, **42** Institute of Biodiversity, Animal Health & Comparative Medicine, **43** Institute of Microbiology and Infection, University of Birmingham,

medRxiv preprint doi: https://doi.org/10.1101/2022.01.03.21268111; this version posted January 3, 2022. The copyright holder for this preprint **(which was not certified by peer review)** is the author/funder, who has granted medRxiv a license to display the preprint in perpetuity.
It is made available under a CC-BY-NC-ND 4.0 International license .

44 Isle of Wight NHS Trust, **45** King's College Hospital NHS Foundation Trust, **46** King's College London, **47** Liverpool Clinical Laboratories, **48** Maidstone and Tunbridge Wells NHS Trust, **49** Manchester University NHS Foundation Trust, **50** Microbiology Department, Buckinghamshire Healthcare NHS Trust, **51** Microbiology, Royal Oldham Hospital, **52** MRC Biostatistics Unit, University of Cambridge, **53** MRC-University of Glasgow Centre for Virus Research, **54** Newcastle University, **55** NHS Greater Glasgow and Clyde, **56** NHS Lothian, **57** NIHR Health Protection Research Unit in HCAI and AMR, Imperial College London, **58** Norfolk and Norwich University Hospitals NHS Foundation Trust, **59** Norfolk County Council, **60** North Cumbria Integrated Care NHS Foundation Trust, **61** North Middlesex University Hospital NHS Trust, **62** North Tees and Hartlepool NHS Foundation Trust, **63** North West London Pathology, **64** Northumbria Healthcare NHS Foundation Trust, **65** Northumbria University, **66** NU-OMICS, Northumbria University, **67** Path Links, Northern Lincolnshire and Goole NHS Foundation Trust, **68** Portsmouth Hospitals University NHS Trust, **69** Public Health Agency, Northern Ireland, **70** Public Health England, **71** Public Health England, Cambridge, **72** Public Health England, Colindale, **73** Public Health Scotland, **74** Public Health Wales, **75** Quadram Institute Bioscience, **76** Queen Elizabeth Hospital, Birmingham, **77** Queen's University Belfast, **78** Royal Brompton and Harefield Hospitals, **79** Royal Devon and Exeter NHS Foundation Trust, **80** Royal Free London NHS Foundation Trust, **81** School of Biological Sciences, University of Portsmouth, **82** School of Health Sciences, University of Southampton, **83** School of Medicine, University of Southampton, **84** School of Pharmacy & Biomedical Sciences, University of Portsmouth, **85** Sheffield Teaching Hospitals NHS Foundation Trust, **86** South Tees Hospitals NHS Foundation Trust, **87** Southwest Pathology Services, **88** Swansea University, **89** The Newcastle upon Tyne Hospitals NHS Foundation Trust, **90** The Queen Elizabeth Hospital King's Lynn NHS Foundation Trust, **91** The Royal Marsden NHS Foundation Trust, **92** The Royal Wolverhampton NHS Trust, **93** Turnkey Laboratory, University of Birmingham, **94** University College London Division of Infection and Immunity**, 95** University College London Hospital Advanced Pathogen Diagnostics Unit**, 96** University College London Hospitals NHS Foundation Trust, **97** University Hospital Southampton NHS Foundation Trust, **98** University Hospitals Dorset NHS Foundation Trust, **99** University Hospitals Sussex NHS Foundation Trust, **100** University of Birmingham, **101** University of Brighton, **102** University of Cambridge, **103** University of East Anglia, **104** University of Edinburgh, **105** University of Exeter, **106** University of Kent, **107** University of Liverpool, **108** University of Oxford, **109** University of Sheffield, **110** University of Southampton, **111** University of St Andrews, **112** Viapath, Guy's and St Thomas' NHS Foundation Trust, and King's College Hospital NHS Foundation Trust, **113** Virology, School of Life Sciences, Queens Medical Centre, University of Nottingham, **114** Watford General Hospital, **115** Wellcome Centre for Human Genetics, Nuffield Department of Medicine, University of Oxford, **116** Wellcome Sanger Institute, **117** West of Scotland Specialist Virology Centre, NHS Greater Glasgow and Clyde, **118** Whittington Health NHS Trust